

**Net Physical Transports, Residence Times, and
New Production for Rivers Inlet, British
Columbia**

by

Michal Hodal

Hon. B.Sc., The University of Toronto, 2007
B.Ed., Ontario Institute for Studies in Education, 2008

A THESIS SUBMITTED IN PARTIAL FULFILMENT OF
THE REQUIREMENTS FOR THE DEGREE OF

Master of Science

in

The Faculty of Graduate Studies

(Oceanography)

The University Of British Columbia

January 2011

© Michal Hodal 2010

Abstract

A hydrographic dataset from the 2008-2009 Rivers Inlet Ecosystem Study (RIES) field program was used (a) to provide a more complete oceanographic description of Rivers Inlet, British Columbia and (b) to develop the first quantitative estimates of estuarine circulation and new production for this system.

Water column observations show a highly stratified two-layer estuarine structure, particularly in the spring and summer months when river discharge and atmospheric heat inputs were high. The net air-sea heat flux had a seasonal range of approximately 220 Wm^{-2} and peaked almost a month earlier in 2008 than in 2009. The main source of river input comes from the Wanonk River. As temperatures begin to rise in the spring, the river discharge can suddenly increase by an order of magnitude (from about $100 \text{ m}^3\text{s}^{-1}$ to almost $1000 \text{ m}^3\text{s}^{-1}$) in less than two weeks.

Residence times (ie. first-order estimates of estuarine circulation) were estimated for every cruise using salinity and temperature budgets in a two-layer box model parameterization of the flow structure. The results show that upper box residence times vary seasonally with river discharge; dropping from about 14 days in the winter to as low as 4 days in the spring at the freshet onset. An earlier flushing event in 2009 caused residence times to drop earlier and could have caused higher advection losses for phytoplankton in the early spring. Overall, residence times averaged to about 7 days for the upper layer and about 165 days for the lower layer during periods of high river discharge, and about twice that during periods of low river discharge. Deep water in the lower layer below the sill was renewed almost once a year in summer and was affected only by vertical diffusion during the rest of the year. Finally, a spring/summer new production estimate of $0.6\text{-}1.7 \text{ gCm}^{-2}\text{d}^{-1}$ (which implies about $110\text{-}300 \text{ gCm}^{-2}\text{y}^{-1}$ assuming no production during the other months) was obtained by combining transport estimates with observations of nutrients to infer a surface nitrate sink. This range compares well with independent estimates made in nearby regions.

Table of Contents

Abstract	ii
Table of Contents	iii
List of Tables	vi
List of Figures	vii
Acknowledgments	ix
Dedication	x
1 Introduction	1
1.1 Research Motivation and Goal	1
1.2 Primary Production from Advective Sources of Nitrate	4
1.3 Research Approach and Outline of Thesis	7
1.4 Methods and Data	9
2 Observation Results	14
2.1 Forcing Factor: Freshwater Input	14

2.2	Forcing Factors: Heat Fluxes	16
2.3	Seasonal Cycle	18
2.4	Estuarine Circulation	21
3	Box Model Analysis	26
3.1	Budget Equations	26
4	Results	31
4.1	Net Transports	31
4.2	Residence Times	32
4.3	New Production	34
4.4	Sensitivity Comparisons	36
4.5	Estimates Using Heat Content	36
5	Discussion	40
5.1	Box Model Estimates: How Much Can We Trust Them? . . .	40
5.2	How do Residence Times Compare with Other BC Fjords? . .	41
5.3	Interannual Variability	42
6	Summary and Next Steps	48
	Bibliography	51
	Appendix A Heat Flux	55
	Appendix B RIES Weather Station	57

Appendix C Catchment Area Calculations	58
Appendix D Monthly Heat Flux Averages	59
Appendix E Hypsometric Curves	61

List of Tables

2.1	Catchment summary	16
5.1	Primary production comparisons with nearby ecosystems . . .	42
B.1	Summary of weather station sensors	57
D.1	Summary of monthly averages for all components of the air-sea heat flux	60

List of Figures

1.1	Map of the British Columbia west coast and Rivers Inlet . . .	3
1.2	Historical returns of the Rivers Inlet sockeye	5
1.3	Simplified model of nitrogen cycling in the surface ocean	6
1.4	Conceptual sequence of thesis outline and objectives.	8
1.5	RIES hydrographic survey map	11
1.6	Conceptual diagram of RIES hydrographic sampling program .	12
2.1	Catchment summary	15
2.2	Freshwater Forcing: (a) Rainfall; (b) Wannock River discharge; (c) salinity time-series at DFO 2	17
2.3	Heat forcing: (a) Atmospheric heat flux; (b) temperture time- series at DFO 2	19
2.4	Deep water renewal	21
2.5	Average salinity transect in May 2009	23
2.6	Average salinity transect in March 2009	24
2.7	CTD profile summary	25
3.1	Conceptual <i>a)</i> flow and <i>b)</i> survey box model for Rivers Inlet .	28
4.1	Summary of (a) input and (b) output paramters in salinity budget	33
4.2	Residence times for the (a) upper and (b) lower boxes	35
4.3	(a) Average nitrate levels and (b) new production estimates in Rivers Inlet	37
4.4	Sensitivity tests of box model estimates	38
4.5	Comparing results with independent estimates using temper- ature budget	39
5.1	Comparing upper residence time estimates for several highly- stratified estuaries along the British Columbia mainland coast	43
5.2	Emperical fit between residence times and river discharge . . .	45

5.3	Historical trend in modelled residence time	47
6.1	Summary of transport estimates and residence times for Rivers Inlet	49
E.1	Hypsometric curve for Rivers Inlet	61

Acknowledgments

During my graduate work I have learned and experienced many new things that I will remember and value for the rest of my life. Thank you to all who have made this possible.

Special thanks to my supervisor, Dr. Rich Pawlowicz for all his academic support and guidance during my graduate studies. Rich, I feel very fortunate to have been the beneficiary of your wealth of knowledge and enthusiasm for oceanography.

To my committee members, Dr. Susan Allen, Dr. Brian Hunt, and Dr. Evgeny Pakhomov, thank you for your honest and helpful insight into my thesis work.

Thank you to all who have made the field work component one of the most memorable parts of my graduate work. In particular, I would like to thank Dr. Brian Hunt (Research Associate and Rivers Inlet Ecosystem Study Project Coordinator), Lora Pakhomova and Chris Payne (Sea Technicians), Asha Ajmani, Jade Shiller, Desiree Tommasi, and Megan Wolfe (fellow graduate students), as well as the Western Bounty crew. Special thanks to the Bachen Family for their amazing hospitality at Dawson's Landing, and to the Tula Foundation for funding this project.

I would also like to thank my waterhole labmates, Neil Swart, Dr. Ted Tedford, Megan Wolfe, as well as Jason McAllister, for all their patience, IT help, and good humour.

Finally I would like to thank my family for all their support. Carla, thank you for your encouragement and unconditional support from day one.

Dedication

To mom and dad. Thank you.

Chapter 1

Introduction

1.1 Research Motivation and Goal

Fjord-type estuaries are a defining feature of the British Columbia (BC) coast. Acting as nutrient traps where river-borne organic and inorganic material collect in concentrated amounts, these systems are generally accepted as regions of high biological productivity that support large populations of mammals, birds, and marine life (Thomson, 1981). Since most of living biomass and mass of nutrients, dissolved gases, and suspended particles are carried by hydrodynamic processes, an essential part in understanding the productivity of an estuarine system is to investigate the net transport of water and its constituents (Dyer, 1991). However, largely in part due to logistical constraints, reasonably detailed investigations of estuarine circulation have been almost exclusively focused in systems situated along the southern part of the BC coast (eg. Strait of Georgia (Li et al., 1999; Pawlowicz et al., 2007), Knight Inlet (Farmer and Freeland, 1983; Stacey et al., 1994), or Alberni Inlet (Hodgins, 1979) situated off the west coast of Vancouver Island). In addition, while general qualitative descriptions of estuarine circulation in estuaries along the central and north part of the coast have been reviewed (eg. Pickard (1961); Thomson (1981)), these reviews are somewhat outdated and provide very limited quantitative information for any one particular system. The lack of more comprehensive studies of estuarine circulation along the central and northern coasts has hampered the evaluation of local, time-dependent processes that drive bio-physical coupling in these systems (Mueter et al., 2002).

Rivers Inlet is a fjord-type estuary situated on the central coast of BC, about 400 km northwest of Vancouver (Figure 1.1). It is about 45 km long by 3 km wide, characterized by steep walls, an rather complicated sill outside

the fjord, and a deep inner basin with maximum depths reaching down to 365 m mid-inlet. It is fed by numerous rivers, and drains into the Queen Charlotte Sound region of the Pacific Ocean. The oceanographic region encompassing Rivers Inlet and the Queen Charlotte Sound is characterized by an unobstructed communication with the Pacific Ocean that is subject to strong climate forcing associated with quasi-steady wind patterns along the coast (Thomson, 1981). Given the dynamic oceanographic setting and the fact that it is relatively devoid of both urban development and oceanographic research, Rivers Inlet is interesting from a purely scientific perspective; however, there are further reasons to investigate estuarine circulation in this system.

Of the approximately 40 inlets that indent the mainland BC coast, Rivers Inlet provides the most dramatic example of an alarming province-wide trend of declining sockeye salmon stocks. For most of the twentieth century, annual returns of Rivers Inlet sockeye averaged over 750 000 fish; trailing slightly behind the Skeena River to produce the third largest catch of this species in British Columbia (McKinnell et al., 2001). However, this once relatively stable sockeye salmon population then underwent an unprecedented decline, falling to less than 1 % of the historical average in 1999 (Figure 1.2). Although the stock has recovered somewhat ($\sim 150\,000$ fish), returns remain well below historic levels and have not returned to harvest levels.

The leading hypotheses for sockeye declines in Rivers Inlet is increased mortality in the early marine phase of their life cycle (McKinnell et al., 2001; Levy, 2006). Spatial covariation among salmon stocks and various coastal oceanographic variables have been observed to decline significantly with distance, implying that survival rates are largely determined by environmental factors over regional scales (< 500 km) (Mueter et al., 2002). Furthermore, as bottom-up forcing is considered to be the primary ecosystem driver along this coast (Ware and Thomson, 2005), one possible cause for poor marine survival are changes in timing and quality of food consumed by juvenile salmon as they migrate through the inlet. Changes in seasonal timing, such as a mismatch between larval occurrence and that of the production of their food, as well as changes in the quality of food have been shown to affect fish stocks in other regions (Beaugrand et al., 2003) and could possibly have similar impacts for this ecosystem (Buchanan, 2007).

The Rivers Inlet Ecosystem Study¹ (RIES) was initiated to study the

¹<http://riversinlet.eos.ubc.ca>

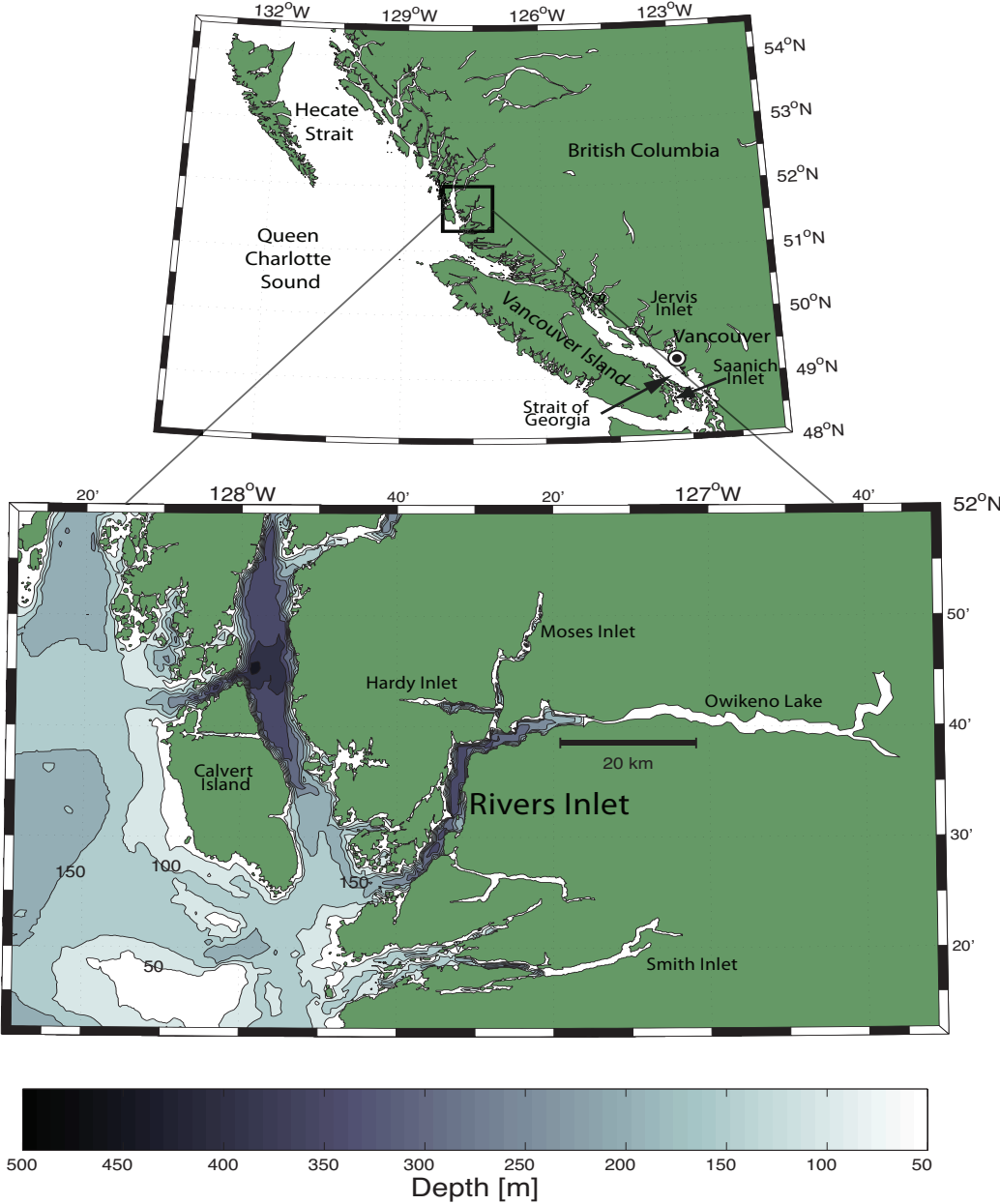


Figure 1.1: British Columbia west coast (upper panel) and Rivers Inlet (lower panel) showing bathymetric characteristics.

factors governing productivity in this ecosystem, focusing mainly on lower-trophic level spring production of plankton. Spring productivity is affected by a complex interplay between biological and physical variables (Sarmiento and Gruber, 2006). An important part in understanding the latter are the hydrodynamic processes that transport water and its constituents (Sarmiento and Gruber, 2006). As part of the RIES, this thesis has the dual, and intrinsically linked goals of obtaining the first quantitative estimates of estuarine circulation and new production in Rivers Inlet. In doing so, we will add new insights into a dynamic region that has been lacking oceanographic research, as well as build on a platform of knowledge that will benefit future, more complex ecosystem modelling.

The conceptual processes that link estuarine circulation to new production are explained in Section 1.2 below. The approach taken to estimate these processes as well as the outline of this thesis is laid out in Section 1.3.

1.2 Primary Production from Advective Sources of Nitrate

In general, primary production of plankton is regulated by the amount of light and nutrients available for photosynthesis (Sarmiento and Gruber, 2006). The most critical nutrient is nitrogen (N), as it is the nutrient that limits production of organic matter in many coastal regions around the world (Sarmiento and Gruber, 2006), and Rivers Inlet in particular (Wolfe, 2010). Phytoplankton growth is driven by nitrogen inputs of two qualitatively distinct sorts; regenerated and 'new' production (Eppley and Peterson, 1979). The difference between the two is in the mechanism of supply and in the chemical form of nitrogen that is taken up in the process (Figure 1.3). Regenerated production is the uptake of a biologically recycled form of nitrogen (ammonium). New production on the other hand depends (for the most part) on mixing and vertical advection processes associated with the circulation of nitrogen in the form of nitrate (Sarmiento and Gruber, 2006). Very little nitrate is recycled in the euphotic zone because nitrifying bacteria, which carry out the process are inhibited by light (Sarmiento and Gruber, 2006). Therefore, a sink of nitrate relative to advected amounts may be interpreted as a first-order estimate of new production (Pawlowicz et al., 2007).

In the literature (eg. Sarmiento and Gruber (2006)), the relationship be-

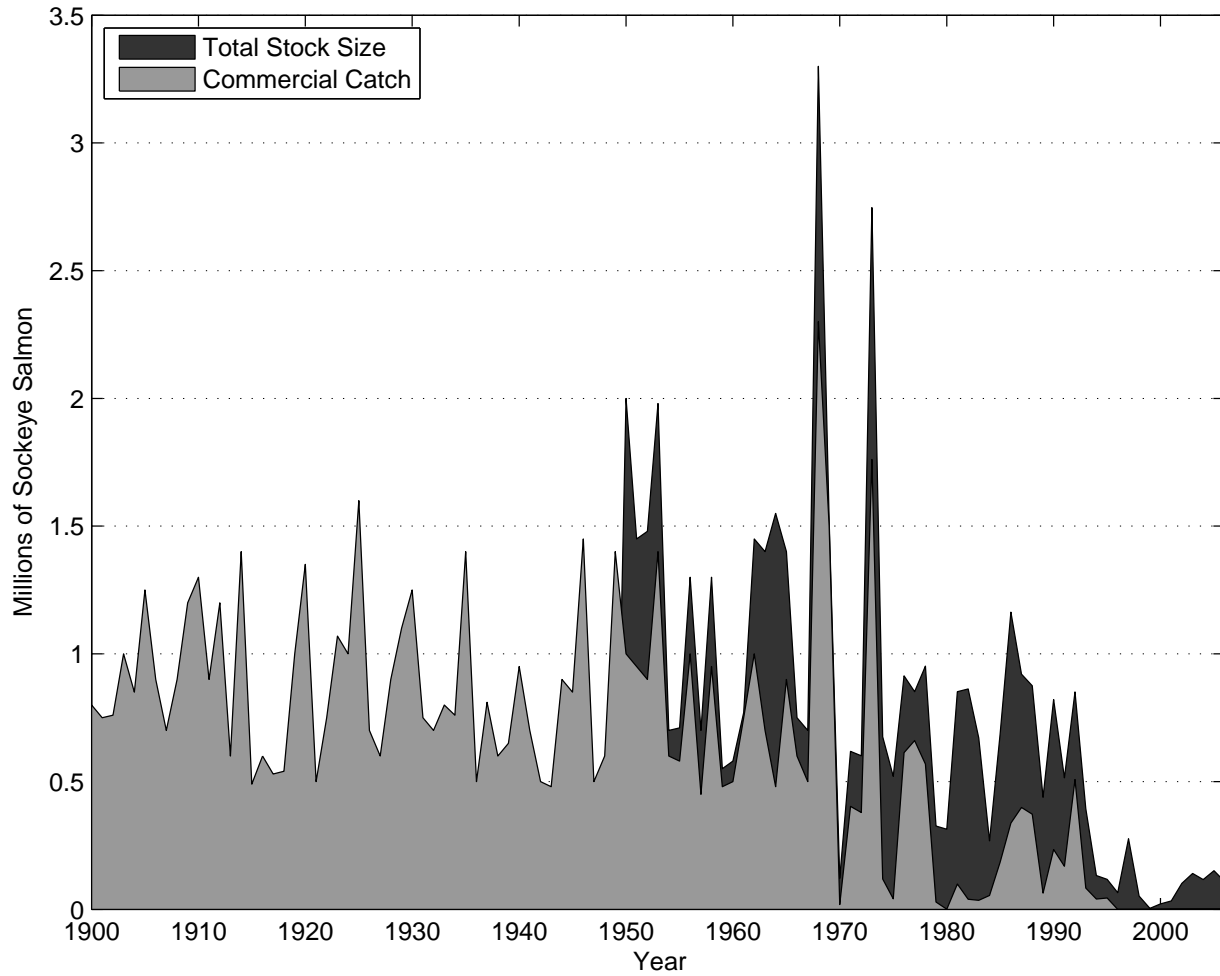


Figure 1.2: Estimates of total stock size (black area) and commercial catch (gray area) of returning adult sockeye salmon to Rivers Inlet. Note: Total stock size estimates were only available from 1948 onwards. Estimates are based on Catch and Escapement figure from RIES website.

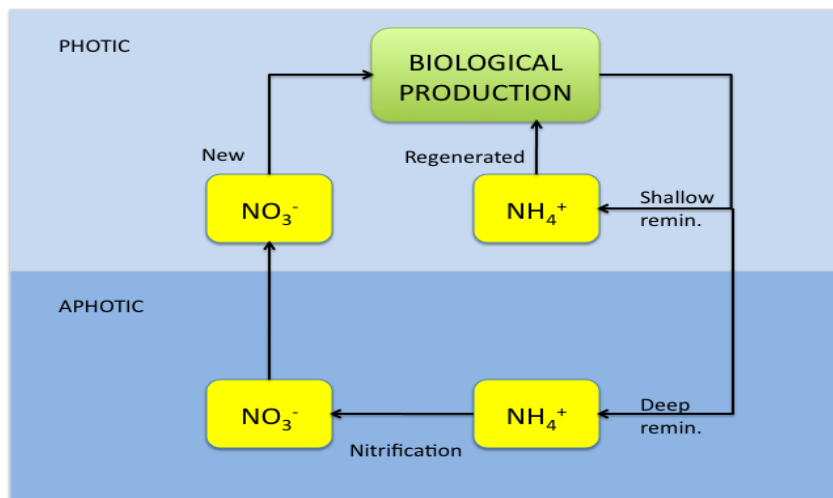


Figure 1.3: Simplified first-order model of nitrogen cycling in the surface ocean. Biological productivity (bacteria, phytoplankton, zooplankton) results from the supply of nitrogen through recycled ammonium (regenerated production) and advection sources of nitrate (new production).

tween new production and the total production (ie. new + regenerated production) is expressed as the f -ratio:

$$f = \frac{\text{New production}}{\text{Primary production}} = \frac{\text{New production}}{\text{New} + \text{regenerated production}} \quad (1.1)$$

Ecosystems with a high physically driven flux of nutrients (eg. many coastal systems) typically show high f -ratios (between 0.7-1.0) because nitrate is mostly supplied from depth whereas the other nitrogen nutrients are regenerated in the euphotic zone (Legendre et al., 1999). This ratio will be used in a later chapter to compare new production estimates with systems where only total production estimates were made (eg. Harrison et al. (1983); Timothy and Soon (2000); Ware and McQueen (2006b)).

1.3 Research Approach and Outline of Thesis

A typical approach taken to investigate advection in estuarine systems is to invoke concepts such as residence times, which are most commonly estimated using simple box models (ie. budgets) (eg. Officer (1980), Gordon Jr et al. (1996), Hagy et al. (2000), Pawlowicz et al. (2007)). Residence time is a first-order analog of advection and is defined as the mean amount of time a parcel of water remains in the estuary once it enters (Hagy et al., 2000). It is, in a sense, the time constant to which all biogeochemical processes are referred to since the total amount of time it takes for water to transit through an estuary often controls the extent to which materials carried in the water can be processed within the system (Sheldon and Alber, 2005).

The method of box models is essentially based on the discretization of a set of linear equations describing tracer and mass balance between a fully mixed control volume and the surrounding environment. The difference ($\Sigma(\textit{sources} - \textit{sinks})$) between imported ($\Sigma\textit{inputs}$) and exported ($\Sigma\textit{outputs}$) materials may be explained by processes within the system (Gordon Jr et al., 1996);

$$\Sigma(\textit{sources} - \textit{sinks}) = \Sigma\textit{inputs} - \Sigma\textit{outputs} \quad (1.2)$$

This thesis is arranged into several sections in accordance with the sequence of steps required in standard box model analysis (Figure 1.4). In the remainder of this chapter, I define the spatial boundaries and provide an overview of sampling logistics and other data sources used in this study (Section 1.4). In Chapter 2, I examine dominant forcing factors and seasonal cycles that determine water column properties and thus, drive estuarine circulation in the inlet. Water column observations of salinity and temperature showed a definite two-layer structure throughout the length of the estuary, particularly in the spring and summer months when river discharge and atmospheric heat inputs were high. Seasonal variations in density were observed in the lower layer; with increasing values (indicating deep water renewal) occurring over the summer months.

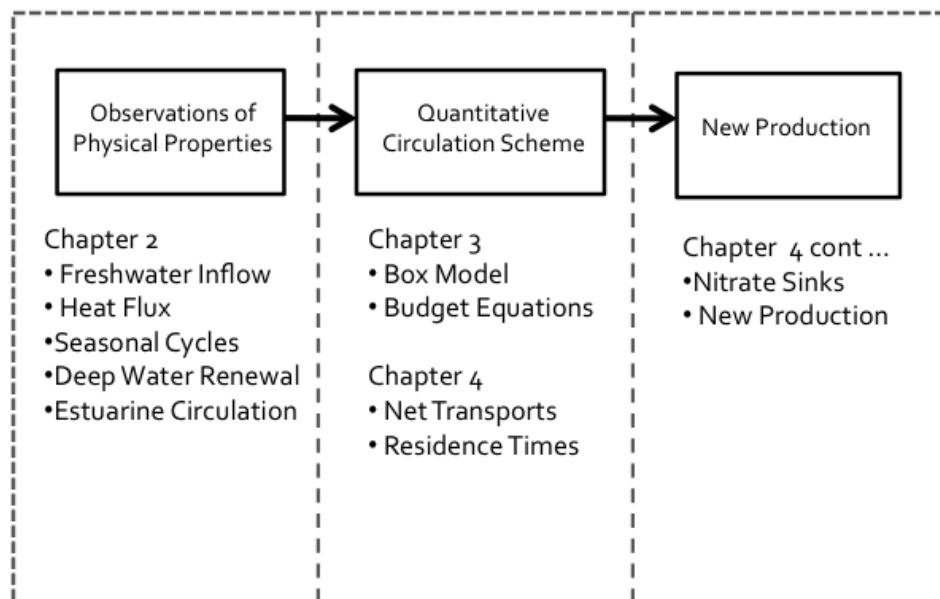


Figure 1.4: Conceptual sequence of thesis outline and objectives.

In Chapter 3 I develop a modified two-layer box model for Rivers Inlet following Officer (1980) and Pawlowicz (2001). This consists of (a) making several assumptions about the flow structure based on earlier observations, (b) using continuity arguments to describe the steady-state balance of mass and tracer concentration, and (c) solving for unknown transport and exchange rates (Section 3.1). We then used both salinity and temperature data independently to obtain estimates of net transports, residence times, and new production in the estuary (Chapter 4). However, estimates using temperature data had several shortcomings, and were therefore reserved for consistency checks of our salinity estimates. Results are quantitative in that numerical values with associated uncertainties are obtained. However, as in all simple models, these estimates are likely biased by neglect of unmodelled processes (Pawlowicz et al., 2007). Thus, these results can be considered as useful first order estimates of estuarine circulation and the net biogeochemical signal relative to the nutrient flux due to physical transport.

In Chapter 5, I discuss the results in light of sensitivity tests, temperature comparisons, and independent new production estimates made in nearby regions (Section 5.1). Furthermore, using basic physical oceanographic data

from Pickard (1961), I estimate residence times for other systems and compare them to Rivers Inlet. The comparisons placed Rivers Inlet in the top spot with the Portland (Naas River) as having the shortest surface residence times. I conclude this section with a discussion on the observed interannual variability in productivity, and on the implications of a trend that suggests an increased impact of surface advection over the last half-century.

Finally, in Chapter 6, I summarize the results with mean circulation schemes and new primary production estimates, and make suggestions for future work.

1.4 Methods and Data

As part of the RIES sampling program, 22 multi-parameter hydrographic surveys were carried out at roughly fortnightly intervals during March through August of 2008 and 2009. All surveys were carried out on the *MV Western Bounty*, a 10 m seine boat. Each hydrographic survey was completed within two days. In this study only stations along a defined transect were used for analysis (Figure 1.5). These stations were chosen to highlight the dominant features inside and outside the inlet.

All *deep* stations included a conductivity-temperature-depth (CTD), dissolved oxygen, transmissometer, and Chlorophyll fluorescence profile to within 15 m of the bottom as well as water samples at 5 m and 30 m depths (Figure 1.6). Water samples were collected using messenger-triggered 2 and 5 L Niskin bottles on the wire above the CTD profiler. Additional surface, 5 m, and 15 m bottle samples were taken at *UBC7*. The most extensive sampling occurred at *DFO 2* (see inset in Figure 1.5). *DFO 2* was the deepest and most representative station of the the inlet. It has also been designated as an important site by other projects in the RIES. At this location bottle samples were taken at surface, 5 m, 10 m, 30 m, 75 m, 100 m, 200 m, and 350 m.

In this study, we take the CTD measured practical salinity as a measure of the true salinity. Although this is not quite correct (Wright et al., 2010), the error incurred is negligible in this estuarine environment. Dissolved O_2 profiles were calibrated with bottle samples analyzed using Winkler titration. Nutrient samples were collected from bottle samples and frozen for later analysis. Chlorophyll *a* (Chl *a*) estimates were made by filtering a known volume

of seawater (between 60 and 300 ml) through a Whatmann GF/F filter. Following standard procedures of Strickland and Parsons (1972), pigments were extracted in 90% acetone for at least 24 hours at -20 °C. These measurements were then used to calibrate the fluorometer readings on the CTD.

In 2009 a number of interpolating *UCTD* stations were added with just CTD casts of the upper 50 m. With the addition of these stations, the along transect sampling resolution of the upper 50 m improved to roughly 2.5 km.

Mean daily Wannock River height levels from gauge 08FA007, as well as a table relating river height levels calibrations to discharge were obtained from Environment Canada (Lynn Campo, personal communication, 2009). An empirical relationship

$$Q_R = -2.6725 (O_L)^3 + 100.46 (O_L)^2 - 102.02 (O_L) + 36.658 \quad (1.3)$$

was derived between the river height levels (O_L) and river discharge (Q_R). Using this relationship, we obtained a daily discharge record from February 21, 1961 to November 22, 2009.

The net heat flux across the air–water interface, H , can be decomposed into four component heat fluxes, namely:

$$H = q_s + q_b + q_h + q_e \quad (1.4)$$

where q_s is the net incoming shortwave solar radiation, q_b is the net longwave radiation, q_h is the net sensible heat flux or direct conduction at the water surface, and q_e is the net latent heat flux of evaporated water, all in Wm^{-2} . Each of these fluxes were computed using the AIR-SEA toolbox as described by Pawlowicz et al. (2001). The AIR-SEA toolbox has a set of routines that codify air-sea fluxes collected from a wide range of scientific literature (Appendix A). For the most part, this study used data from the RIES weather station to calculate heat flux terms.

The RIES weather station site is located near *DFO 2* on a small island approximately 30 km from the head: Latitude 51.5486 N, Longitude 127.5316 W (Figure 1.5). In March 2009, the existing *Ethel* weather station (SFU) was replaced by a new (UBC) weather station *Laska* (Appendix B). By juxtaposing measurements from both stations, we have obtained an approximately two year meteorological dataset for Rivers Inlet. Availability of certain measurements varied due to lack of sensors or mechanical problems but for the most part hourly records for solar radiation, wind speed and direction, and

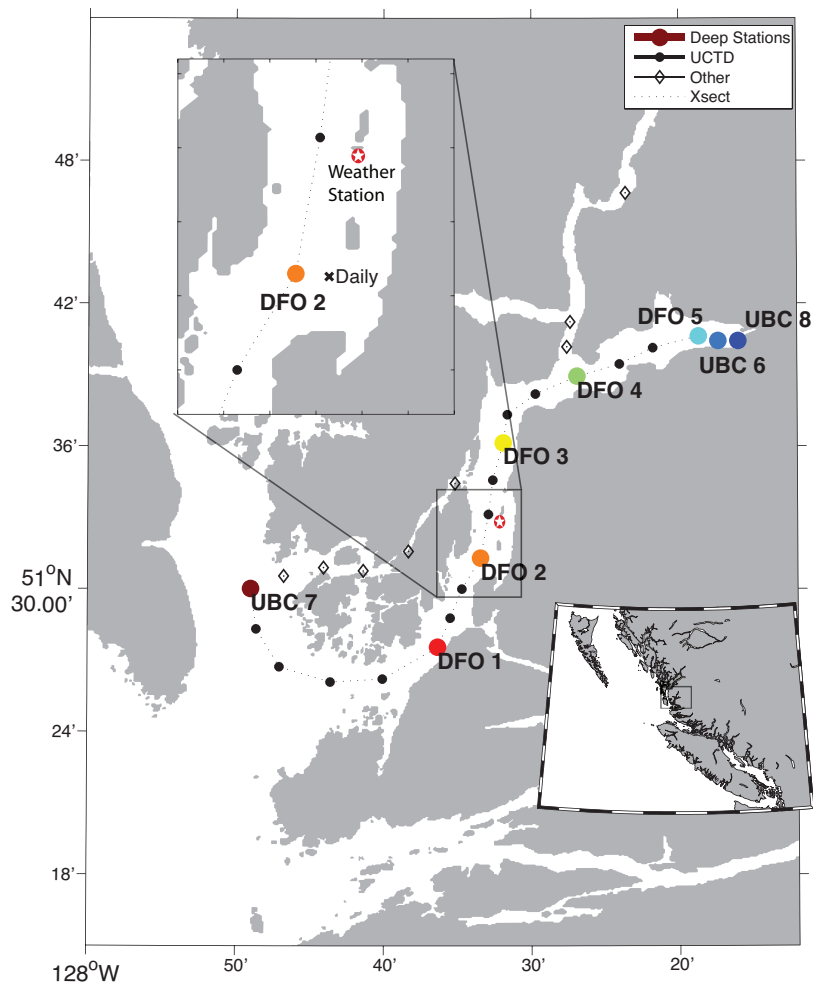


Figure 1.5: RIES hydrographic survey summary: All *deep* and *UCTD* stations along the transect (dotted line) are labeled by name and small black dots, respectively. *UCTD* stations were added for the 2009 sampling year and include only *CTD* casts of the upper 50 m (see Figure 1.6). Stations that were not used for analysis here but were also sampled during RIES surveys are represented by diamonds. Inset shows a zoom in of *DFO 2* (site of most extensive sampling, see text), *daily* sampling site, and the RIES weather station.

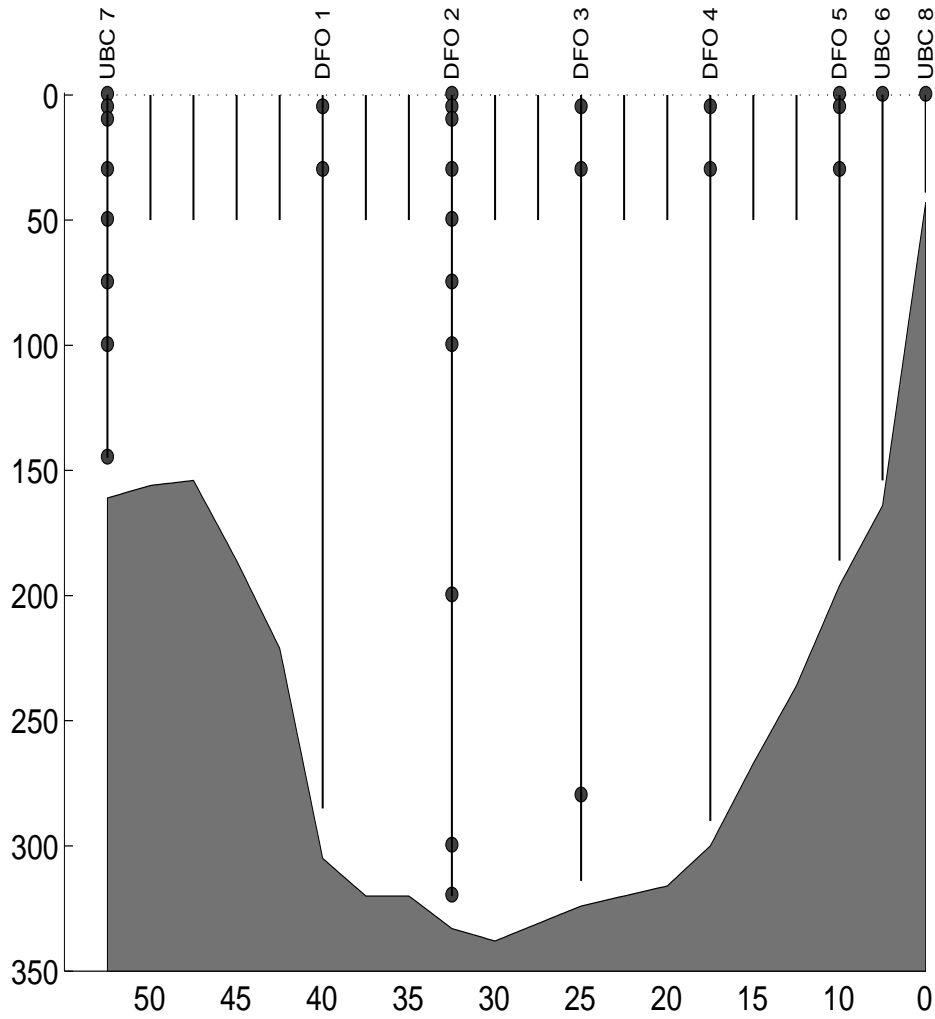


Figure 1.6: Conceptual diagram of RIES hydrographic sampling program showing CTD casts (solid line) and bottle samples (circles) along the thalweg of the inlet. CTD casts ranged from 20 m to 360 m. Bottle samples and deep casts were only taken at *deep* stations (labeled above). UBC 7 was the station farthest from the head and best representation of waters outside the estuary. Lines in between deep stations represent UCTD casts taken in 2009.

temperature were available for both years. Surface water temperature measurements were required for estimating longwave, sensible, and latent heat fluxes. The monthly surface water temperatures were calculated by averaging bi-weekly surface temperatures taken at the *DFO 2* sampling station. Since field surveys were only conducted March through August, linearly interpolated estimates were used for calculating the longwave, sensible, and latent component of air-sea heat flux during the winter months. Similarly, an interpolated shortwave estimate was used for the month of May 2008 and May 2009 when the RIES weather station was not operational.

Chapter 2

Observation Results

2.1 Forcing Factor: Freshwater Input

Catchment Area

The largest and only gauged inflow of freshwater into Rivers Inlet comes from Owikeno Lake (see Figure 1.1). This lake has a surface area of approximately 89 km² and discharges westwards into the head of Rivers Inlet via the Wannock River. The Wannock River is approximately 6.5 km long, with a mean channel width of approximately 100 m. The fraction of the total inflow into Rivers Inlet that is represented by Wannock River inflow was analyzed using comparisons of surface area against other catchments that drain into Rivers Inlet (Appendix C). The drainage basin for Owikeno Lake is outlined by *Area 1* in Figure 2.1. It has an estimated area of 3970 km² and alone represents approximately 65% of the total catchment of all areas draining into Rivers Inlet (see Table 2.1). This catchment basin is further inland and is substantially higher in elevation than the other catchments. It also has more than 85% of the total glacial concentration of all catchments areas added together. This results in greater storage of winter precipitation and likely increases the impact of total percentage of flow from this catchment during the spring and summer months when high altitude snowmelt is dominant.

Catchment outlined by *Area 2* drains into Rivers Inlet predominantly via Kibella Bay located close to the head (see Figure 1.1) and is a notable source by area and percentage of glacial concentration (Table 2.1). Located down-inlet, *Area 3* and *4*, while similar to *Area 2* by area, are lower in elevation and have less winter precipitation storage and glacial coverage. The impact of these catchment areas are therefore likely to be smaller year-round, and

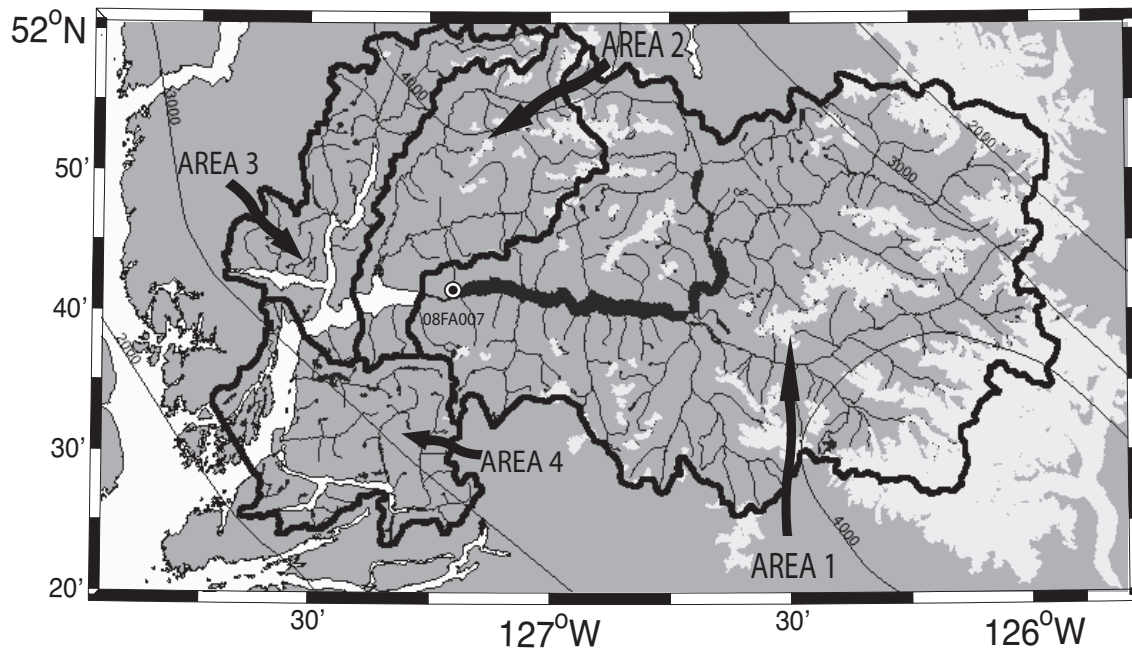


Figure 2.1: Outlines of four main catchment areas that drain into Rivers Inlet. Also shown are all rivers, glaciers, and large scale annual precipitation averages (in mm) from the Land and Resource Data Warehouse (LRDW) database (Appendix C). Gauge 08FA007 measures discharge from catchment *Area 1* and is maintained by Environment Canada.

particularly minimal during the spring freshet.

Freshwater Inflow

Annual cycle of flow discharge at Wannock River was observed to be typical of nearby systems having stored runoff inflow characteristics (Pickard, 1963) (Figure 2.2*b*). In both years, lowest flow values were recorded during the winter months; this was particularly true during the cold and dry winter of 2008/2009 when record low discharge values (less than $60 \text{ m}^3\text{s}^{-1}$) persisted throughout the month of March. At the beginning of spring, increasing temperatures and daylight create favorable conditions for the first spring freshet. In mid-May 2008 the impact of the freshet was dramatic. Discharge values at Wannock River increased by an order of magnitude (from about $100 \text{ m}^3\text{s}^{-1}$ to almost $1000 \text{ m}^3\text{s}^{-1}$) in just one week. The freshet onset in 2009

	Catchment Area (A_i)	Percent of Total Catchment	Percent of Total Glacial Concentration
Area 1	3970 km ²	65 %	> 85%
Area 2	820 km ²	13 %	< 10%
Area 3	590 km ²	10 %	< 5%
Area 4	790 km ²	12 %	< 1%

Table 2.1: Catchment summary of Figure 2.1.

was less pronounced and characterized by an earlier but smaller ($\sim 500 \text{ m}^3\text{s}^{-1}$) peak in late April caused by local storm activity. Following the freshet onset, average flows remain high (approximately $564 \text{ m}^3\text{s}^{-1}$) throughout the spring and summer months. Flow variability during the spring and summer months was also high. A pattern of sharp increases reaching over $650 \text{ m}^3\text{s}^{-1}$ and lasting anywhere from one to two weeks followed by below average discharge was evident in both years.

The flow begins to gradually drop in late summer and early fall. Weaker fall and winter flows are sometimes interrupted by sharp and relatively short-increases. Peaks in the fall of both years reached well over $1000 \text{ m}^3\text{s}^{-1}$ and were due to heavy rainfall from intense storms that recorded as much as 100 mm of cumulative rain per day (Figure 2.2a).

The cumulative annual precipitation at the RIES weather station was approximately 2300 mm and consistent with precipitation estimates over regional scales (Figure 2.1). Assuming similar rainfall in the Owikeno catchment and multiplying by the catchment area of 3970 km^2 , we get an annual precipitation runoff of about $9 \times 10^9 \text{ m}^3\text{y}^{-1}$. This value compares well with annual river discharge means of $320 \text{ m}^3\text{s}^{-1}$ or $10 \times 10^9 \text{ m}^3\text{y}^{-1}$ and suggests a level of consistency between the river gauge and precipitation data.

2.2 Forcing Factors: Heat Fluxes

A well defined seasonal signal was observed in the net heat flux estimates (Figure 2.3a). The seasonal signal is due principally to variations in short wave radiation. During the 1.5 year long record, the net monthly shortwave

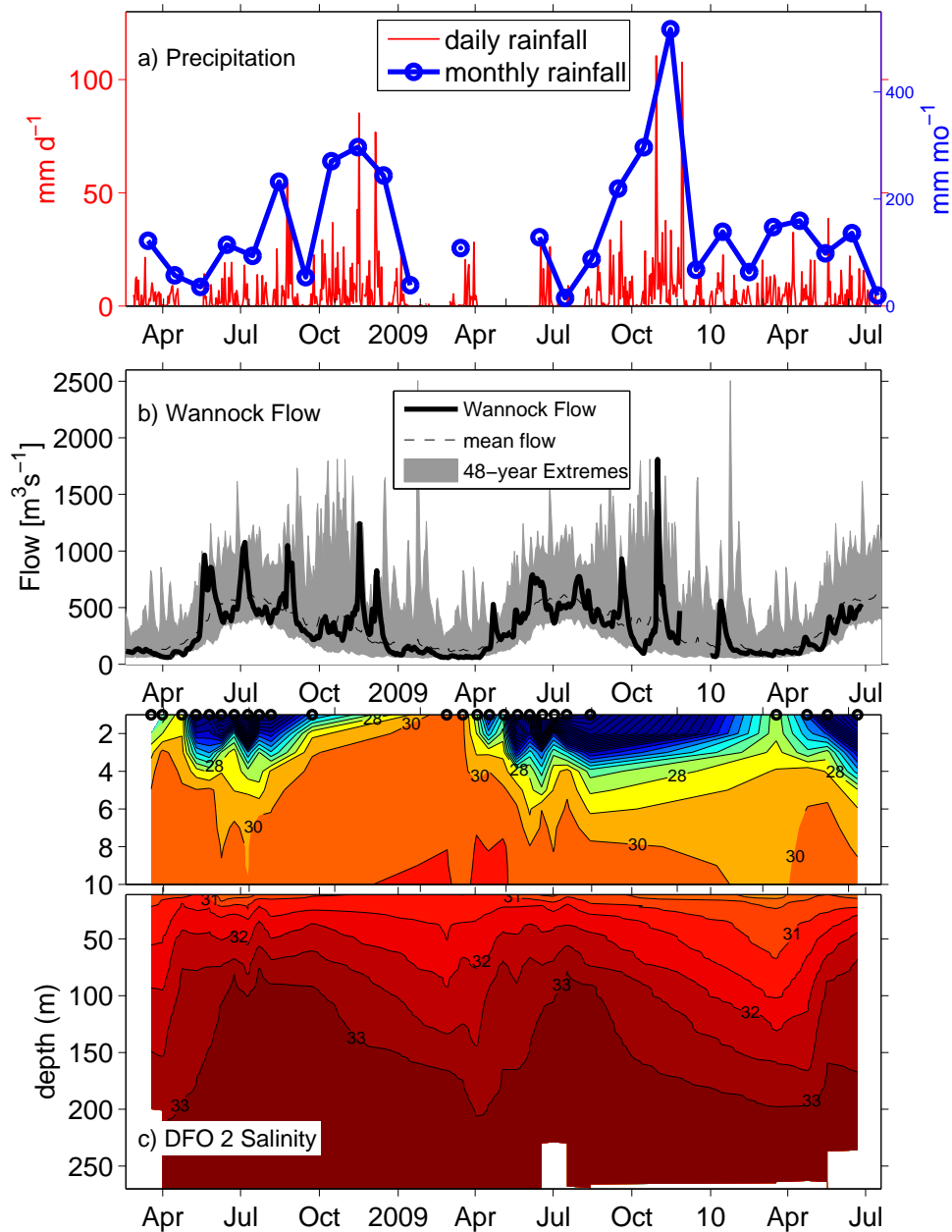


Figure 2.2: Freshwater forcing: (a) rainfall measured at RIES weather station; (b) Wannock river flow (shaded region is 48-year extremes, dashed line indicate annual averages, diamonds represent cruise dates); (c) salinity time-series contours at DFO 2 (circles at 0 m indicate survey dates). Note the change in vertical scale in figure (c).

flux reached a maximum of approximately 240 Wm^{-2} in July 2009 and a minimum of approximately 20 Wm^{-2} in the previous winter. Comparing between the two summers, 2009 monthly means peaked at about 60 Wm^{-2} higher than in 2008 due to a full two-week stretch of sunny weather during late July of that year.

The net sensible and latent fluxes vary proportionally to wind speed with higher values in the winter and lower values in the summer. Throughout the year, these fluxes were relatively small and slightly negative, averaging annually to a net loss of approximately -5 Wm^{-2} and -15 Wm^{-2} , respectively. Net longwave fluxes vary with season and are in the range of -50 to -80 Wm^{-2} . Day-to-day variability is quite high for shortwave fluxes but for the other three components of the flux, daily means do not differ significantly from monthly means.

The net air-sea heat flux has a seasonal range of approximately 220 Wm^{-2} and peaked almost a month earlier in 2008 than in 2009. Peak values were higher in 2009 (170 Wm^{-2}) than in 2008 (107 Wm^{-2}). Tabulated monthly values for all components of the heat flux are summarized in Appendix D.1. The annual heat flux mean was estimated at 10 Wm^{-2} into the water implying that Rivers Inlet is a small net exporter of heat to the outside coastal waters. The annual mean calculated here, albeit slightly higher, is in close agreement with value of 5 Wm^{-2} computed by Pawlowicz et al. (2007) for nearby Strait of Georgia.

2.3 Seasonal Cycle

Surface layer salinities over the two year sampling period at *DFO 2* are well correlated with the seasonal cycle of freshwater discharge (Figure 2.2c). Periods of high river discharge caused very high stratification of the water column. During this period, salinities at *DFO 2* (which is almost 30 km down inlet) were observed to increase from nearly 0 at the surface to as much as 30 in just the upper 5 m. During the winter months, when river discharge subsided and surface layer mixing was induced by storm activity, large vertical salinity gradients vanish and surface salinities almost reached deeper layer values.

A close relationship was also observed between the net air-sea heat flux and surface temperatures (Figure 2.3b). Similar to heat flux observations,

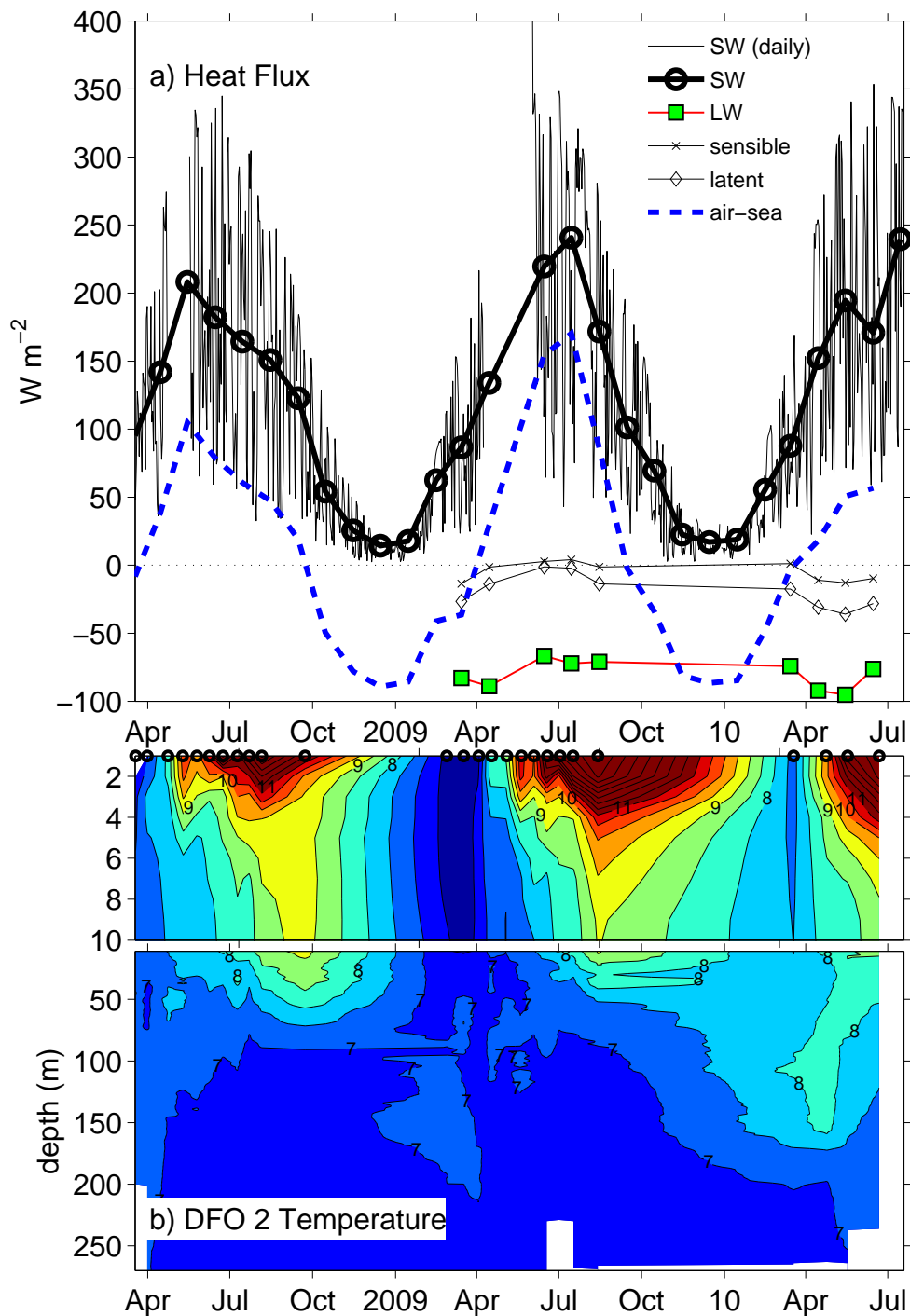


Figure 2.3: Heat forcing in Rivers Inlet: a) monthly means of important terms in the air-sea heat flux; where SW=net shortwave, LW=net longwave heat terms b) temperature time-series contours at DFO 2 (circles at 0 m indicate survey dates). Note the change in vertical scale.

water surface temperatures peaked earlier and were lower in 2008 than in 2009. In 2008 water surface temperatures peaked at 12.8 °C compared a peak of 14.8 °C recorded in 2009.

Salinity and temperature values below the upper layer of the water column were observed to be more uniform but still varied seasonally. Figure 2.4 shows the changes in deep water properties at 270 m in the central basin from 2008-2010. The pattern of density changes appears identical at both *DFO 2* and *DFO 3* (Figure 2.4a). An increase in lower layer densities was observed during the summer months and this can only happen with the inflow of dense bottom water from outside the estuary (Pawlowicz et al., 2007). The explanation for this pattern of summertime deep-water renewal (DWR) is well documented. Briefly, prevailing northerly winds along the BC coast during the summer months cause off-shore Ekman transport (Thomson, 1981). This results in coastal upwelling of dense waters that flow onto the regional shelves and sometimes into the deep basins of nearby estuaries as gravity currents (Dyer, 1997). As the heavier water comes in, it sinks down and increases the density near the bottom. Examples of other systems that renew in this fashion include the Strait of Georgia (Masson, 2002; Pawlowicz et al., 2007), Knight Inlet (Stacey, 1985) on the mainland north of the Strait of Georgia, and Saanich Inlet (Anderson and Devol, 1973) on the south-east side of Vancouver Island.

In addition to the large scale forcing, DWR also depends on local features such as sill depth, tides, and mixing rates (Farmer and Freeland, 1983). Rivers Inlet, Strait of Georgia, Knight Inlet, and Saanich Inlet also share the common feature of having a relatively deep sill (>60 m).

At the onset of a renewal period, the first water that flows in is slightly higher in oxygen because it's source in the North Pacific is closer to the surface where oxygen levels are higher (Figure 2.4b). As heavier water enters (upwelled from greater depths), average oxygen levels decrease. In the winter months lower layer densities and oxygen levels gradually decrease as freshwater mixes down and respiration uses up O₂. Minimum density values occurred in the spring during both years, but fell lower in 2008 than in 2009. Lower deep basin density values in the spring can increase the gradient between outside upwelled source waters and can therefore cause stronger renewal events. Based on inter-annual observations of density, deep water

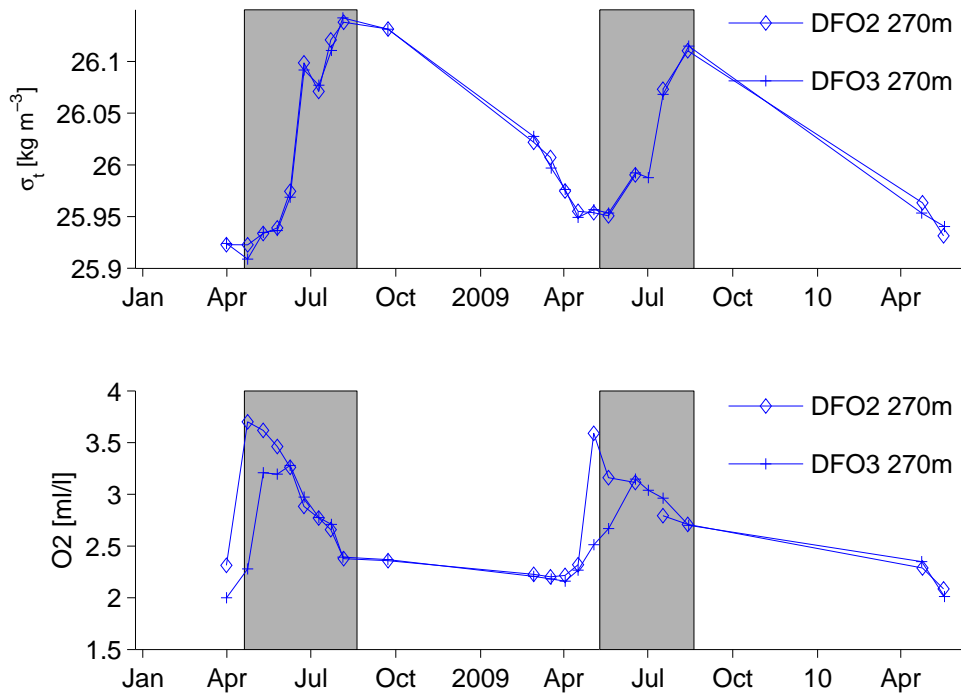


Figure 2.4: Variations in Rivers Inlet deep water: a) density and b) oxygen. Periods of renewal are shaded.

renewal was earlier and stronger in 2008 than in 2009.

2.4 Estuarine Circulation

During the spring and summer months a very thin layer of freshwater stratifies the upper water column along the entire length of the estuary (Figure 2.5). Slight along-channel variations in surface salinity were observed especially around *DFO3* and likely reflect the small addition of freshwater from Moses Inlet. Typical salinity values during this time were near 0 at the surface and increased to about 20 in just the top few meters of the water column. Water column stratification during typical winter conditions was much weaker but still present (Figure 2.6). Over the full vertical scale, the large majority of seasonal variation of salinities were within the top 5 m

of the water column (Figure 2.7a). For temperature, while largest seasonal variations were also observed to be mostly within the top 5 m, there was still considerable seasonal variation observed below this depth (Figure 2.7b).

In general, water in the upper layer was observed to be more saline towards the mouth. This is the result of a vertical entrainment process across the interface, resulting from velocity shear between the upper and lower layers (Dyer, 1974). As water is entrained vertically, a compensating inflow of water enters the estuary from the subsurface (Thomson, 1981). Due to the compensating subsurface inflow, lower layer salinities were close to salinity values observed in the outside shelf region of the estuary.

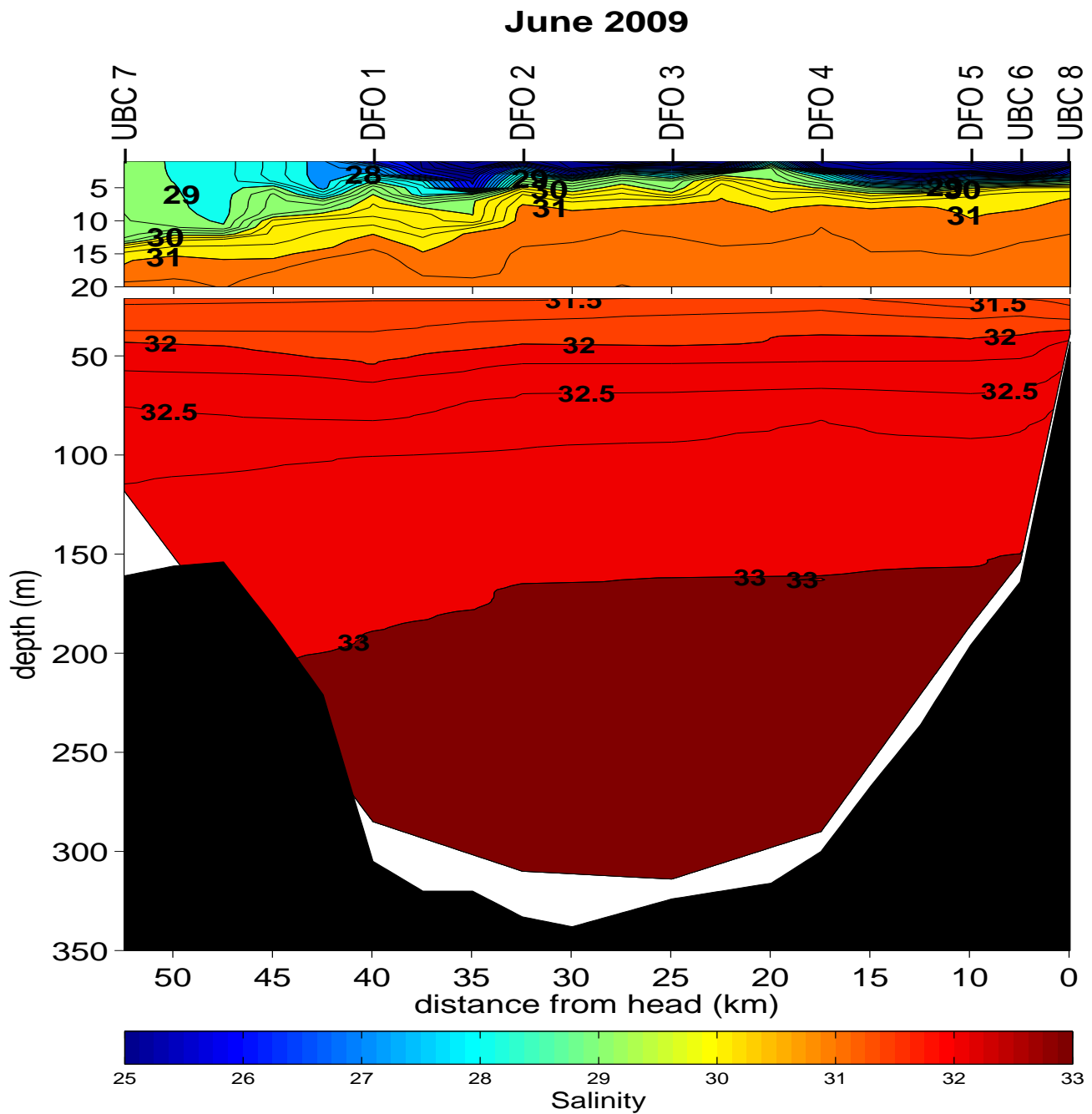


Figure 2.5: Average salinity transect in May 2009. Average Wannock River discharge during this time was well above $500 \text{ m}^3\text{s}^{-1}$. Note the change of depth scale.

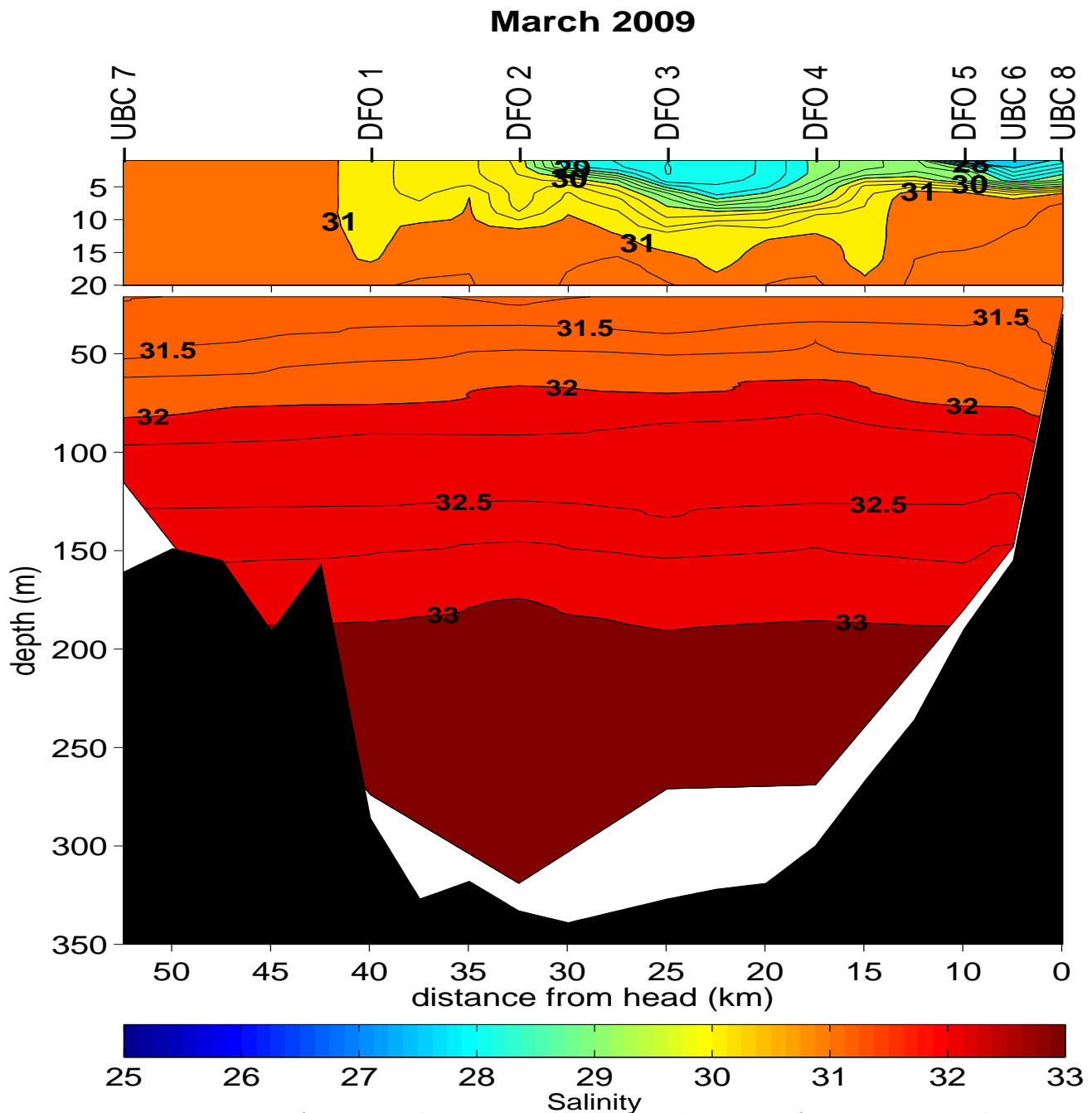


Figure 2.6: Average salinity transect in March 2009. Average Wannock River discharge during this time was about $80 \text{ m}^3\text{s}^{-1}$. Note the change of depth scale. Colorbar range was kept identical to Figure 2.5 for comparison purposes.

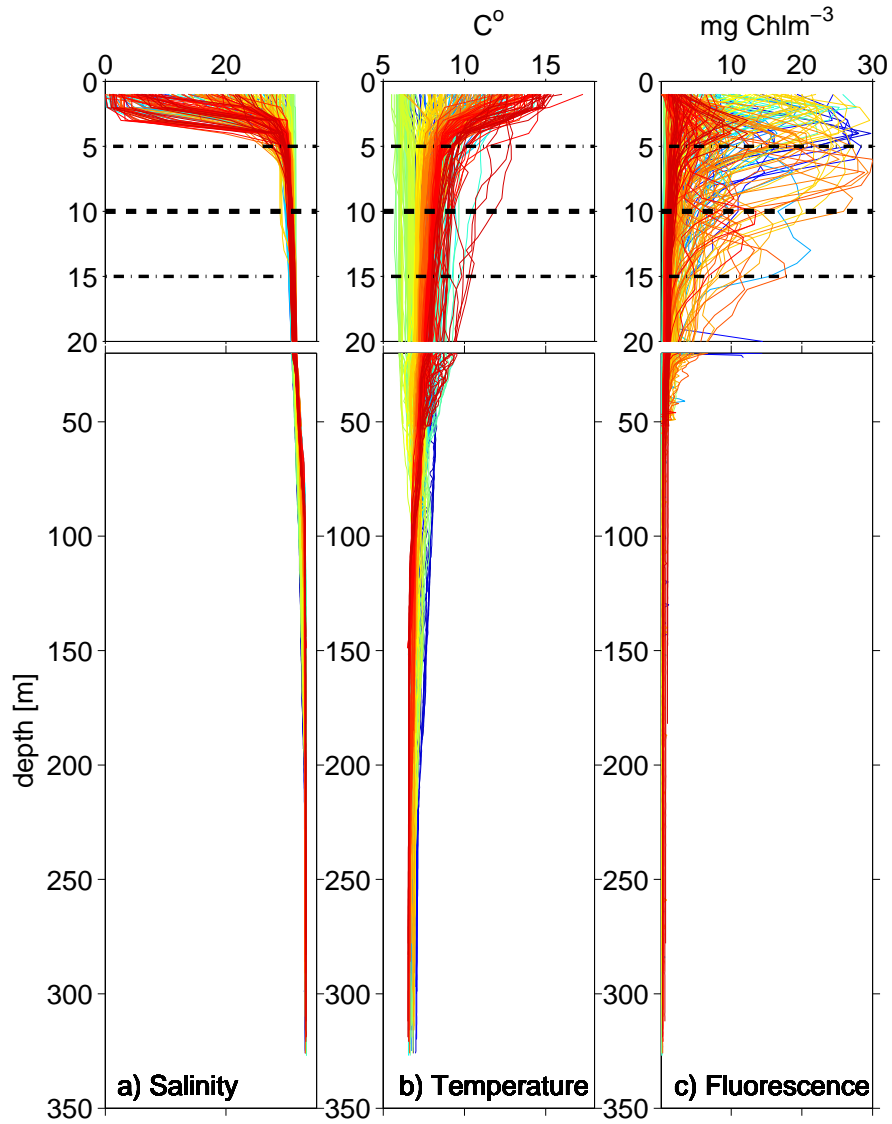


Figure 2.7: All CTD profiles of (a) salinity; (b) temperature; (c) Chlorophyll fluorescence. Dashed lines indicate interface depths in sensitivity comparisons (see Chapter 4). Different colors are used to distinguish between other profiles.

Chapter 3

Box Model Analysis

In this section a general mass and tracer budget is developed for Rivers Inlet. I use both salinity and temperature data independently to obtain estimates of net transports and residence times in the estuary. However, estimates using temperature data had several shortcomings (Section 3.1), and were therefore reserved for consistency checks of our estimates based on salinity data (Chapter 4).

3.1 Budget Equations

A box model parameterization of the flow structure for Rivers Inlet is illustrated in Figure 3.1*a*. The assumed pattern of water flow and exchange, as well as the boundaries of this system were chosen on the basis of observed physical properties, estuary dimensions, and sampling logistics described in the previous section. The estuary is represented by one basin which was split into an upper box and a lower box at a depth of 10 m. The volume for each box is assumed to be constant at time scales of interest (i.e. sub-tidal).

The 10 m depth of this horizontal interface was chosen as the best representation of both physical and biological features in the inlet. The ultimate purpose for the box-model developed here was to obtain estimates of both residence times and new production. A choice of 5 m, while a better representation of the physical stratification, would miss a significant part of the biological signal since high values of Chlorophyll fluorescence were observed below this depth (Figure 2.7c). This would therefore affect the new production estimates (Figure 4). Variation and sensitivities of box model estimates based on the choice of interface depth are discussed in Section 5.1.

Advection terms for fluxes into and out of the upper box include freshwater inflow from the Wannock River Q_r , vertical entrainment from the lower box Q_w , and horizontal outflow Q_u . Non-advective vertical exchange E_l and

E_u (a parametrization of mixing effects) between the boxes are assumed to be equal in magnitude and opposite in direction and therefore cancel each other out in the overall mass budget. Note that we must have a nonzero E_u term to explain the winter-time rise in lower-box density (Figure 2.4a). Non-advective horizontal exchange terms are assumed to be negligible compared to horizontal advective terms. This assumption is typical of two-layer systems that are dominated by high river flow and is also required to avoid an under-determined system (Hagy et al., 2000). Given these assumptions, the general tracer balance for the upper box of volume V_u is:

$$Q_r\theta_r + Q_w\theta_l + E_l\theta_l - E_u\theta_u - Q_u\theta_u + F = V_u \frac{\partial\theta_u}{\partial t} \quad (3.1)$$

where θ_r is the tracer concentration of the freshwater input; θ_u and θ_l are tracer concentrations in the upper and lower box, respectively; and F represents an external source of tracer. For example, if the tracer is temperature, then

$$F = \frac{a_s H}{\rho c_p} \quad (3.2)$$

and represents the addition of atmospheric heat flux H over a surface area a_s normalized by a nominal density ρ and heat capacity c_p following Pawlowicz and Farmer (1998).

Advective flow for the lower box is assumed to be uni-directional because the system is closed by walls of the fjord. This implies that all inflowing ocean water from Queen Charlotte Sound Q_{qc} is (eventually) entrained into the upper box. As in the previous case, we assumed non-advective exchange for the lower box was only across the horizontal interface. Given these assumptions, tracer budget for the lower box of volume V_l is:

$$Q_{qc}\theta_{qc} - Q_w\theta_l - E_l\theta_l + E_u\theta_u = V_l \frac{\partial\theta_l}{\partial t} \quad (3.3)$$

Finally, having already assumed that non-advective water exchange between layers is equal and opposite (ie. $E_u = E_l = E$) and all inflowing ocean water is entrained into the upper box (ie. $Q_{qc} = Q_w$), we can express the water budget as:

$$Q_r + Q_{qc} - Q_u = 0 \quad (3.4)$$

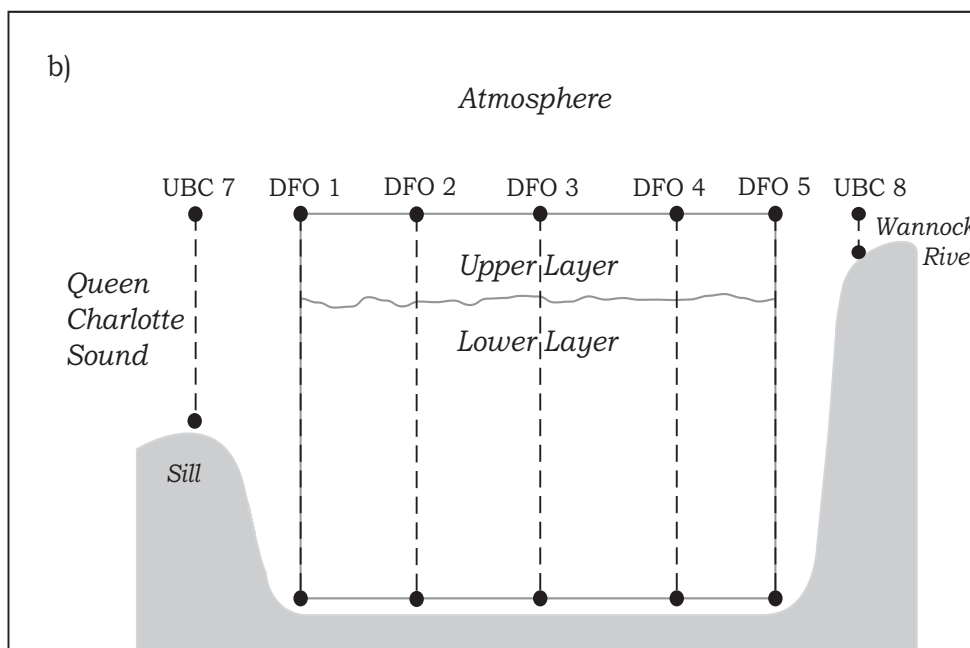
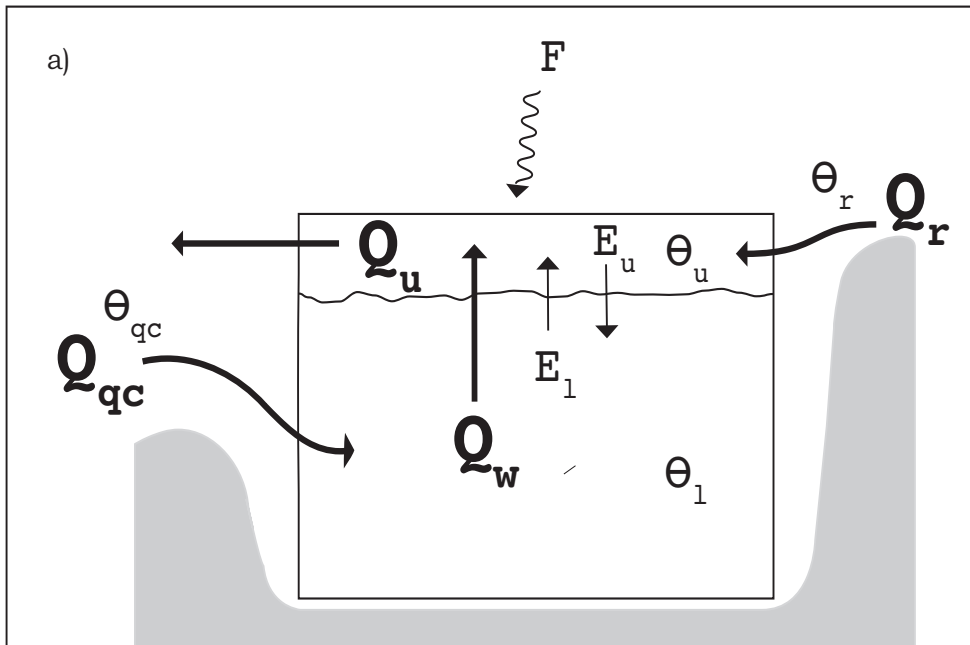


Figure 3.1: Conceptual a) flow and b) survey box model for Rivers Inlet. Advection terms for fluxes into and out of the upper box include freshwater inflow from the Wannock River Q_r , vertical entrainment from the lower box Q_w , and horizontal outflow Q_u . Non-advective vertical exchange E_l and E_u (a parametrization of mixing effects). Inflow into the lower box comes from shelf waters of the Queen Charlotte Sound is represented by Q_{qc} . Tracer concentrations of the Wannock River θ_r , upper θ_u and lower θ_l box, and outside source waters θ_{qc} are also shown. Finally, F represents an external source of tracer into the surface layer.

Equations 3.1-3.4 describe the tracer field for the assumed flow structure in Rivers Inlet. Solving these equations for the unknown flow parameters gives:

$$Q_u = \frac{Q_r(\theta_{qc} - \theta_r) - F + V_l \frac{\partial \theta_l}{\partial t} - V_u \frac{\partial \theta_u}{\partial t}}{\theta_{qc} - \theta_u} \quad (3.5)$$

$$Q_{qc} = \frac{Q_r(\theta_u - \theta_r) - F + V_l \frac{\partial \theta_l}{\partial t} - V_u \frac{\partial \theta_u}{\partial t}}{\theta_{qc} - \theta_u} \quad (3.6)$$

$$E = \frac{\theta_l - \theta_{qc}}{\theta_u - \theta_l} \cdot Q_{qc} \quad (3.7)$$

Figure 3.1*b* illustrates a conceptual survey model representation of the system. Water properties inside each box were calculated by averaging over all *DFO* stations. The basin was closed at *DFO* 1; the last *deep* station inside the estuary. Station *UBC* 7 was the farthest site sampled outside of Rivers Inlet and was the best representation of outside oceanic 'source' waters. On a few occasions, sampling at *UBC* 7 was missed due to inclement weather and linearly interpolated values were used. Freshwater discharge was also required; we used the daily Wannock River gauge discussed previously in Section 2.1.

When salinity S is used as a tracer (ie. $\theta = S$), the terms θ_r and F in Equations 3.5-3.7 are zero, and no additional data is required. Furthermore, the storage terms $V_l \partial S_l / \partial t - V_u \partial S_u / \partial t$ in Equations 3.5-3.7 were found to be much smaller (by an order of magnitude) compared to $Q_r S_{qc}$ and $Q_r S_u$, and could be ignored in our calculations. Therefore, using salinity data and assuming steady-state, Equations 3.5-3.7 simplify to:

$$Q_u = \frac{S_{qc}}{S_{qc} - S_u} Q_r \quad (3.8)$$

$$Q_{qc} = \frac{S_u}{S_{qc} - S_u} Q_r \quad (3.9)$$

$$E = \frac{S_l - S_{qc}}{S_u - S_l} \cdot Q_{qc} \quad (3.10)$$

This system of equations is similar to the 'Knudsen' relations that have long been used in circulation estimates; the difference being that we keep the E term to account for non-advective exchange. The simplicity of the Knudsen equations has also made it the standard for estimating budgets in other systems where in situ data is limited (Gordon Jr et al., 1996), and may therefore serve as a useful way to compare our results with other fjords along the BC coast.

Having calculated the atmospheric heat flux in Section 2.2, we were also able to estimate flow parameters in Equations 3.5-3.7 using temperature. However, our analysis was far more limited using a temperature budget. First, the estimates had significantly higher error bars due to the additional uncertainty carried over by the heat flux terms. Second, the two-layer box model was a weaker representation of the temperature distribution in the inlet, particularly in the winter which caused unrealistic estimates. And third, river temperature data, a major requirement in the budget, was only available for the 2009 sampling season.

Chapter 4

Results

4.1 Net Transports

Estimates of net transports were made by applying Equations 3.8-3.10 for each cruise. In order to do so, time series of box average temperature and salinity were required. Average salinities were calculated for the upper and lower box, and Queen Charlotte ocean source waters (Figure 4.1*a*). Salinities in the lower box (S_l) were slightly lower (higher) in the summer (winter) but well correlated with source waters outside the estuary (S_{qc}). Lowest S_l value of 32.0 was recorded in March 2008. During summer DWR, S_l values were observed to increase for both years, peaking at 32.9 in July 2009. Salinities in the upper box (S_u) were far more variable but correlated with freshwater discharge (Figure 4.1*b*). Highest S_u values in the range of 28-31 were recorded during the late winter months when river discharge and estuarine stratification was low. With the onset of the spring freshet, salinity values in the upper box can drop very rapidly. In May 2009, a salinity drop of 29 to 25 was observed within a time-span of about two weeks. Note that these values represent averages in the upper 10 m layer; salinity values at 0 m (ie. surface) can drop far below 25. Low S_u values persist throughout periods of high river discharge. Period of high river discharge ($Q_r > 250 \text{ m}^3\text{s}^{-1}$) and low S_u value ($S_u < 28$) are represented by the shaded areas and span May 20 - Aug 20, 2008 and May 3 - Aug 15, 2009.

The resulting outputs of advective and non-advective coefficients are shown in Figure 4.1*b*. The two advective flows Q_u and Q_{qc} differ only by the value of Q_r as required by Equation 3.4. The pronounced peaks in calculated flows in early May 2008 resulted from a high Q_r value being divided by a relatively smaller difference of salinities (i.e. denominator terms in Equa-

tions 3.5 and 3.6). On average, highest advective transports occurred during the summer months when river discharge was high (shaded region in Figure 4.1). Some inter-annual variability during this period was observed. The average outflow Q_u for the shaded regions were $2.66 \pm 0.30 \times 10^3 \text{ m}^3\text{s}^{-1}$ in 2008 compared to a lower average of $2.08 \pm 0.10 \times 10^3 \text{ m}^3\text{s}^{-1}$ in 2009.

Advection values during the winter months when river discharge was low were approximately $0.72 \pm 0.10 \times 10^3 \text{ m}^3\text{s}^{-1}$ and were much smaller than summer values. Non-advective vertical exchange coefficients (E) were at least an order of magnitude smaller than the surface or subsurface inflow, averaging to approximately $0.75 \pm 0.10 \times 10^3 \text{ m}^3\text{s}^{-1}$ year-round.

4.2 Residence Times

Residence times τ_u (τ_l) for the upper (lower) boxes were calculated using

$$\tau = \frac{V}{\sum Q} \quad (4.1)$$

where V represents the volume and $\sum Q$ the net inflow into the respective boxes. Estimates for box volumes, calculated from the hypsometric curve of Appendix E, were $V_u = 1.343 \times 10^9 \text{ m}^3$ and $V_l = 24.618 \times 10^9 \text{ m}^3$.

Residence time magnitudes varied seasonally and changed rapidly with the onset of the freshet. For example, upper box residence times for periods of high river discharge (shaded regions in Figure 4.2a) averaged 7 days with a minimum value of approximately 4 days in May 2008. In contrast, values for τ_u during periods of low river discharge ($Q_r < 100 \text{ m}^3\text{s}^{-1}$) were at times observed to be almost 3 times higher, reaching approximately 18 and 22 days in March 2009. Largest fortnightly changes in residence times were observed during the early spring months and coincided with changes from low to high river discharge. During these shifts residence times were observed to decrease by an average rate of 5 days per week for both years.

The similar pattern between residence times in the upper and lower boxes was directly related to the similar pattern in Q_u and Q_{qc} which drive the variability in residence time calculations. Error bars for residence time calculations were obtained using bootstrapping techniques following Pawlowicz (2001). Briefly, the method was based on taking individual CTD casts and

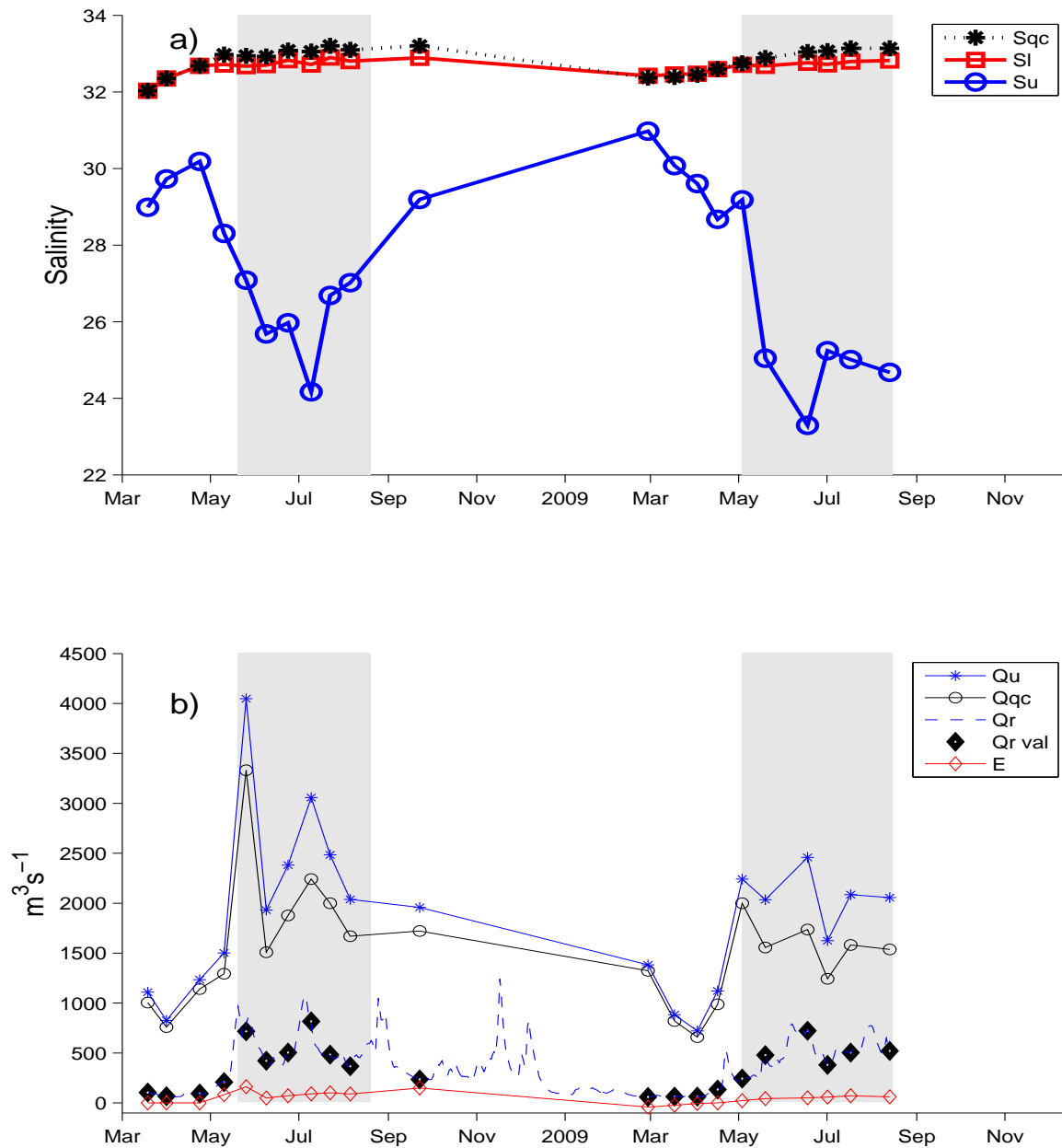


Figure 4.1: Summary of (a) input and (b) output parameters in salinity budget: Source water salinities S_{qc} were slightly higher but compared well with lower layer salinities S_l . Upper layer salinities S_u dropped significantly at the onset of the freshet (shaded regions). Also showing upper layer outflow Q_u , source water inflow Q_{qc} , and exchange coefficients E . Black diamond on the daily river discharge (dotted lines) curve indicate discharge values used during cruise dates.

resampling them a number of times with replacement. These bootstrap replicates are then used to calculate transport parameters using the equations above. Finally, error bars are calculated by taking the standard error of the resulting bootstrap replicates of transport estimates. Since these error bars only reflect the inherent variability in the dataset and do not include other source of error, eg. in calculating box volumes, the actual errors of residence time estimates were higher but correlated across all estimates. Therefore, the error bars in Figure 4.2 show the importance of the effects of errors that were set by the observations.

4.3 New Production

Estimates of new production (P_{new}) (Figure 4.3) were made by interpreting the sink of nitrate in the upper box as biological productivity (see Section 1.2 for an explanation). The relevant budget for advective source of nitrate into the upper box is:

$$P_{new} = N_l Q_w - N_u Q_u \quad (4.2)$$

where N_u (N_l) is the average nitrate concentration in the upper (lower) box. Riverine nutrient inputs were ignored since they were somewhat smaller than the uncertainties in this calculation, and were only available for part of the sampling season. Nitrate levels for the upper and lower boxes are shown in Figure 4.3a. Note that N_l and N_u represent box averages over relevant depths and sampling stations (refer to Figure 1.6). Differences in nitrate levels between the two boxes were smallest in the winter. Variability of N_l was observed to be small throughout the year; much of it likely due to measurement error. Upper box nitrate levels dropped in the spring and remained low ($5 - 8 \mu\text{M}$) throughout the summer months.

The box-average nitrate concentrations were combined with earlier advective transport in Equation 4.2 to estimate P_{new} (Figure 4.3), converting to carbon units using the Redfield C:N ratio of 106:16 and normalizing by the surface area. The two-year average of P_{new} during the spring and summer months was $1.3 \text{ gCm}^2\text{d}^{-1}$. Taking this value as the representative rate of new production during the spring/summer and assuming no new production the rest of the year yields an annual P_{new} average of about $230 \text{ gCm}^2\text{y}^{-1}$

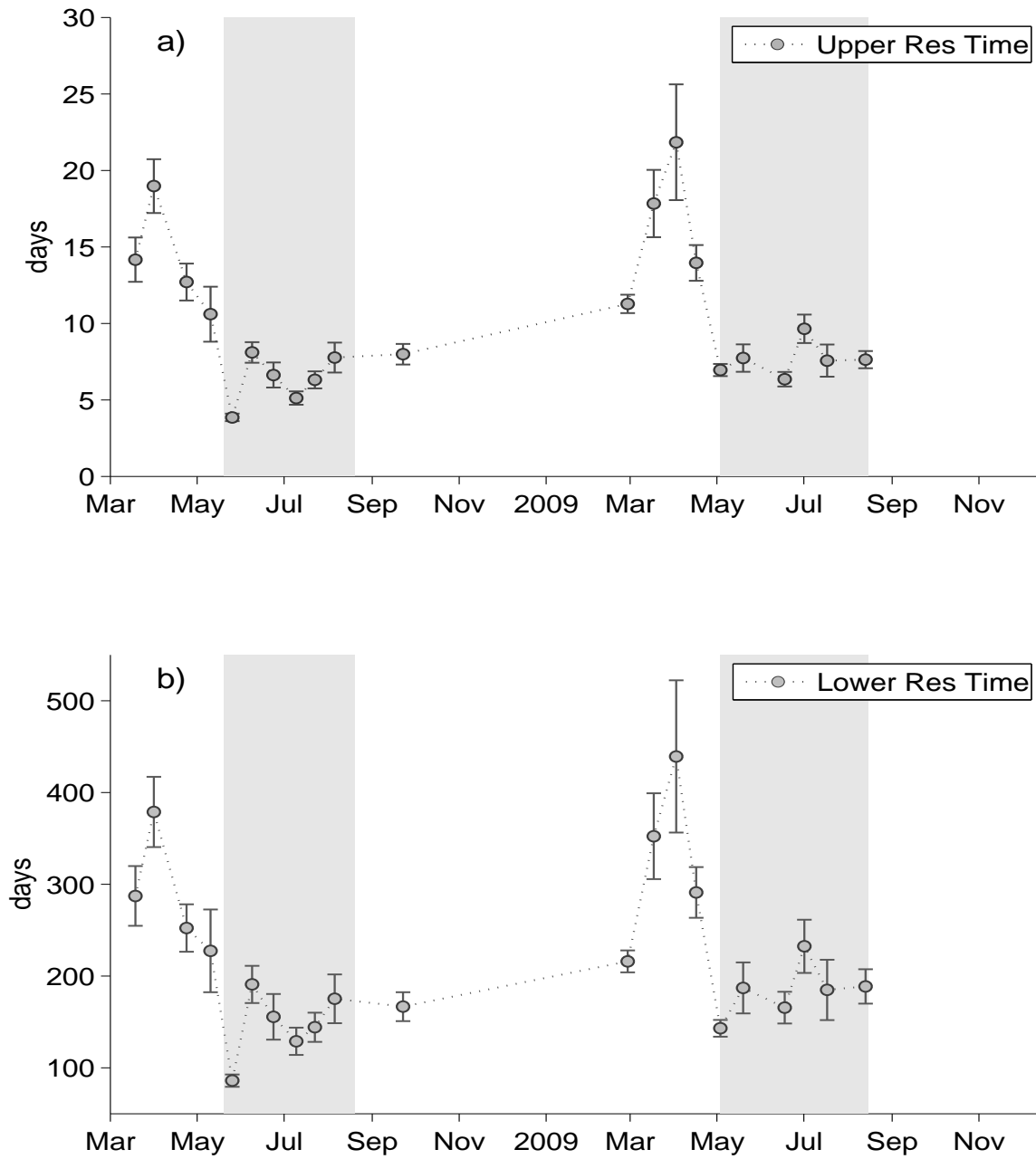


Figure 4.2: Residence times for the (a) upper and (b) lower boxes with error bars from bootstrap samples (see text). Shaded regions indicate periods of high river discharge.

(with more than 50% uncertainty carried over from nutrient and transport estimates).

4.4 Sensitivity Comparisons

To examine the sensitivity of the results to the choice of interface depth, upper layer residence time and new production estimates were calculated using two different interface depths: a shallower 5 m interface; and a deeper 15 m interface (Figure 4.4). The choice of a shallower interface depth resulted in shorter residence times (by about a day in the summer and about 5 days in the winter), while a deeper interface depth resulted in longer residence estimates (by about the same amount) (Figure 4.4a) .

New production estimates varied very little in the winter months, but varied by as much as a factor of two depending on interface depth (Figure 4.4b). A shallower interface resulted in lower new production values, while a deeper interface resulted in higher ones.

4.5 Estimates Using Heat Content

Parameters using Equations 3.5-3.7 and corresponding residence times using Equation 4.1 were also calculated using observations of water temperature, and the atmospheric heat flux estimates from Section 2.2. Overall, there was reasonable agreement in a one-to-one comparison of residence time using the two independent methods (Figure 4.5). Most residence time estimates were within a day of the one-to-one comparison. The largest deviations were observed to occur with longer residence times associated with winter periods. During this time, residence time values deviated by as much as 8 days, with shorter estimates coming from the temperature budget.

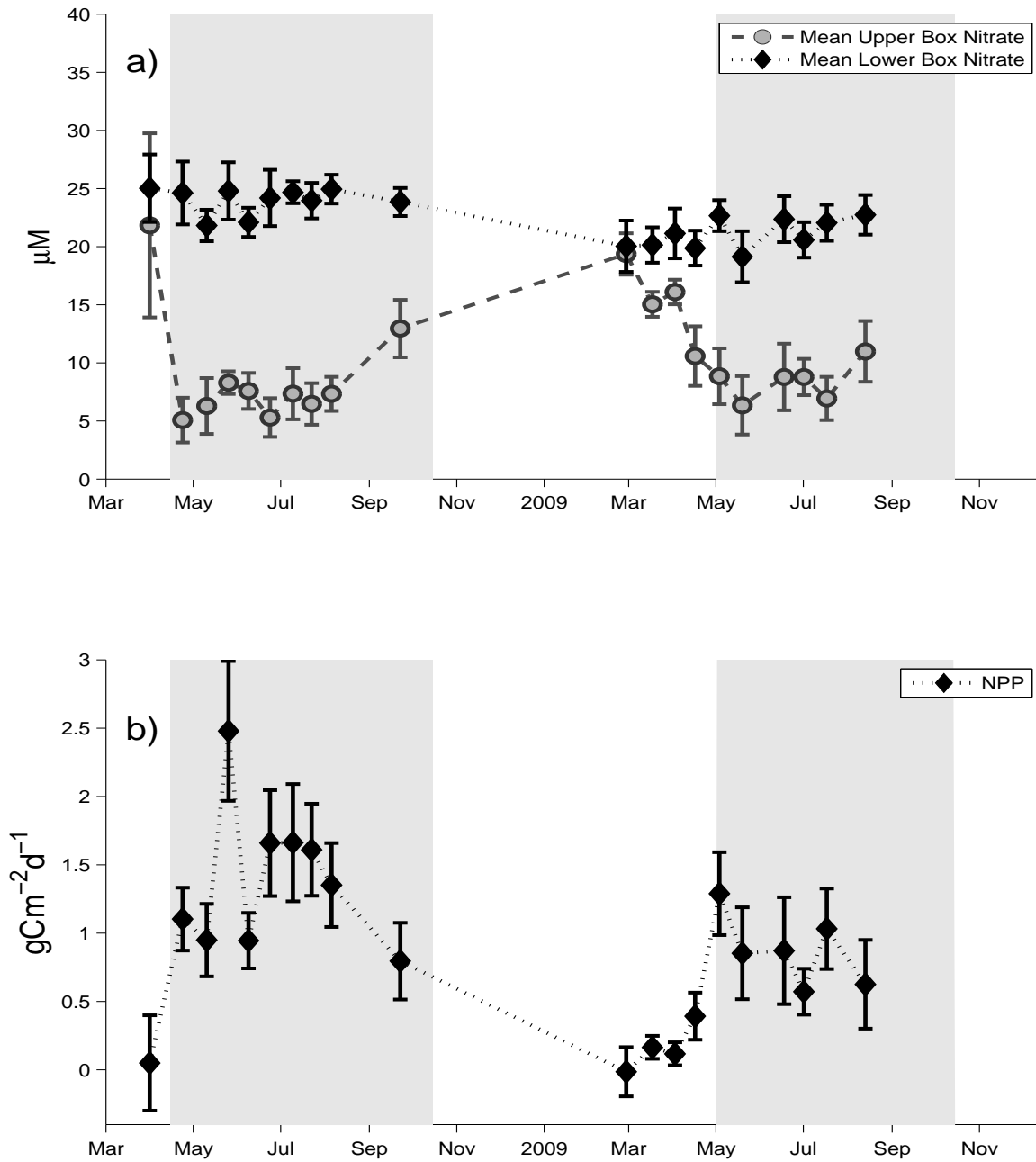


Figure 4.3: (a) Average nitrate levels in upper and lower boxes; and (b) new production estimates in Rivers Inlet. Also shown is the period of higher new production (shaded region).

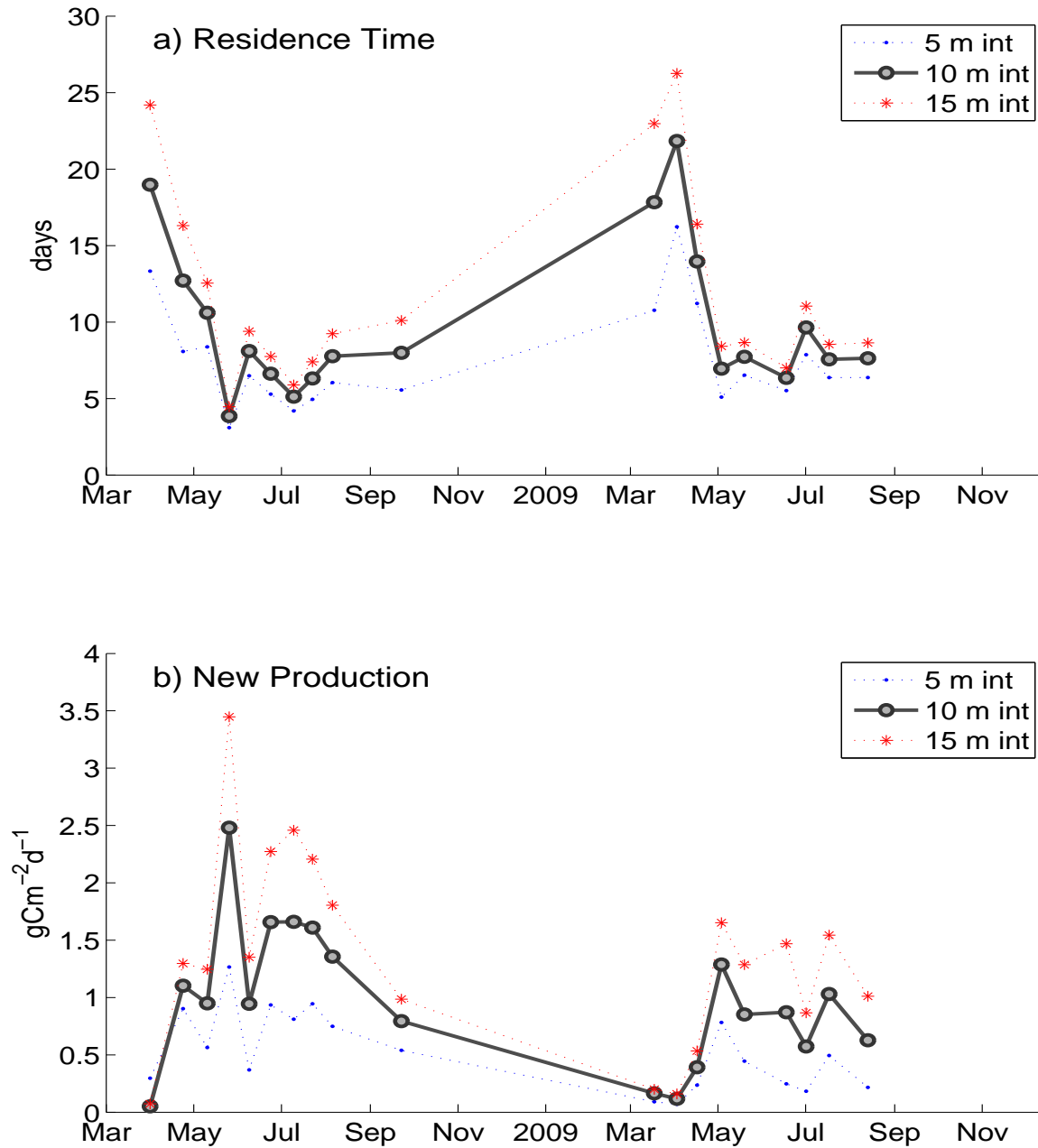


Figure 4.4: Sensitivity tests of box model estimates: shown are (a) upper residence time and (b) new production estimates using 5 m, 10 m, and 15 m interface depths.

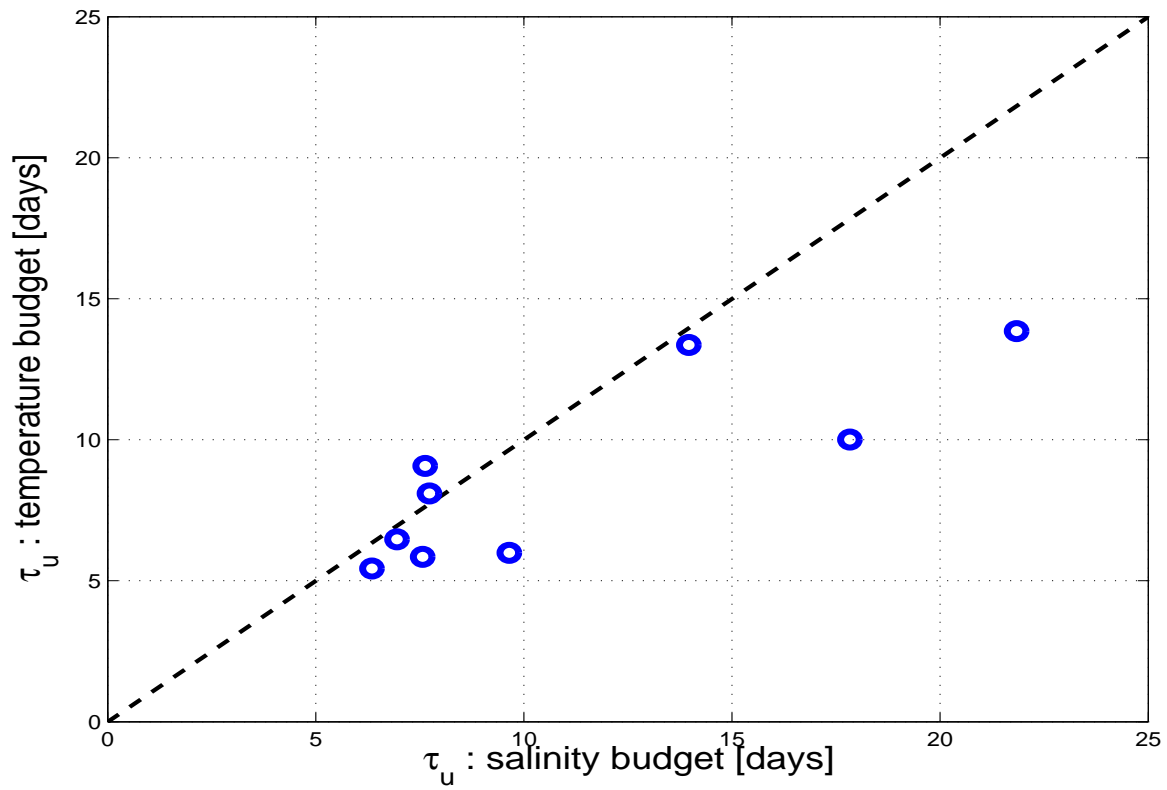


Figure 4.5: A one-to-one comparison (dashed line) of 2009 upper residence times (τ_u) using a salinity and temperature budget.

Chapter 5

Discussion

5.1 Box Model Estimates: How Much Can We Trust Them?

This study was the first to estimate estuarine circulation and new production in Rivers Inlet. Since it was the first, we could only validate our estimates with: (a) sensitivity tests; (b) independent estimates using different tracers; and (c) production estimates from areas that were in reasonable geographic proximity and in more or less the same oceanographic domain.

Our sensitivity tests (Figure 4.4a) suggested that residence times were not significantly sensitive to our choice of interface depth. Differences of ± 1 day in the summer and ± 5 days in the winter were still within the range of uncertainty in our summer/winter estimates. Furthermore, independent estimates of residence time using a temperature budget also showed similar results (Figure 4.5). For the most part, residence time using the two methods were within about 15 % of each other. Larger differences occurred during the winter months when flows and water stratification were low. With a less robust two-layer approximation of the flow structure, model predictions were more uncertain during the winter period.

New production estimates were more sensitive to our choice of interface depth, particularly during the summer months, but were still within the approximately 50 % uncertainty for these estimates (Figure 4.4b). The full range of mean seasonal new production estimates was between 0.6-1.7 $\text{gCm}^2\text{d}^{-1}$. Assuming half-a-year of production (ie. multiplying this range by 180 days) gives an annual average of about 110-300 $\text{gCm}^2\text{y}^{-1}$.

Estimates of primary production using independent methods have been published for only a handful of ecosystems near Rivers Inlet (Table 5.1). In one study, Ware and McQueen (2006b) used a climate-forced nutrient, phy-

toplankton, and zooplankton model to estimate primary production for the Hecate Strait (see Figure 1.1). The model was forced by various climate factors that regulate phytoplankton growth through water temperature, hours of sunlight, wind mixing and coastal upwelling. Overall the model suggested that primary production in the Hecate Strait Region ranged between 141-278 $\text{gCm}^2\text{y}^{-1}$. In the same study, having no information about the physical circulation of the region, a highly oversimplified equation attempting to capture the essence of nitrogen upwelling (i.e. new production) was used in part to estimate a regional f-ratio of 0.82. Taking this ratio with the estimated production suggests an annual average new production range of 116-230 $\text{gCm}^2\text{y}^{-1}$ for the Hecate Strait region, and compares well with estimates obtained here.

In other studies, various ^{14}C -uptake methods have been used to estimate primary production in the Strait of Georgia (280 $\text{gCm}^2\text{y}^{-1}$) (Harrison et al., 1983), Saanich (490 $\text{gCm}^2\text{y}^{-1}$) and Jervis Inlets (290 $\text{gCm}^2\text{y}^{-1}$) (Timothy and Soon, 2000). Assuming these to be approximate measures of gross production, and taking an f-ratio of about 0.7 as reasonable for coastal marine ecosystems (Legendre et al., 1999) this would suggest our annual average were in the mid-range of these ecosystems. Therefore, on the basis of a reasonable match with independent estimates of nearby systems, it appears that the circulation scheme developed here does well in predicting new production values in Rivers Inlet.

5.2 How do Residence Times Compare with Other BC Fjords?

Comparing our residence time estimates with other systems can be useful, for example, in ranking the relative strength of surface advection in Rivers Inlet on a larger scale. However, with the exception of the Strait of Georgia, no published estimates of residence times in systems along the coast were found. The only viable approach was to make estimates based on physical data published in Pickard (1961) (Figure 5.1). Thus I will make estimates based on very limited data, the inlets that were chosen for comparison was a subset of all inlets classified by Pickard (1961) as having a distinct two-layer vertical salinity-depth profile due to high river runoff at the head.

In Equations 3.8 and 4.1, the outside source salinity was assumed to be 33;

Region	Primary Production Estimate	New Production
Rivers Inlet		110-300 gCm ⁻² y ⁻¹
Strait of Georgia	280 gCm ⁻² y ⁻¹ (Harrison et al., 1983)	
Hecate Strait	141-278 gCm ⁻² y ⁻¹ (Ware and McQueen, 2006b)	116-230 gCm ⁻² y ⁻¹ (suggested)
Saanich Inlet	490 gCm ⁻² y ⁻¹ (Timothy and Soon, 2000)	
Jervis Inlet	290 gCm ⁻² y ⁻¹ (Timothy and Soon, 2000)	

Table 5.1: Primary production comparisons with nearby ecosystems. New production value for the Hecate Strait was estimated using an f-ratio calculated in (Ware and McQueen, 2006b).

a reasonable assumption based on deep layer salinities observed in all inlets. Upper layer salinities were more variable. To account for the variability, a range of values (between 22-26) was used. Furthermore, upper 10 m volume estimates were based on length, and mean width values reported in Pickard (1961). Finally, discharge values were estimated annual means which were also from Pickard (1961).

The overall comparisons placed Rivers Inlet and the Portland canal (Naas River) as having the shortest surface residence times among all systems (Figure 5.1). All of the systems with comparable outflow rates were much bigger in volume. Put another way, Rivers Inlet has the unique feature of having very high surface advection for its relatively small size. This suggests that Rivers Inlet is significantly impacted by surface advection, more so than most other inlets along this coast.

5.3 Interannual Variability

Productivity: 2008 vs 2009

The seasonal mean of new production was about 40% higher in 2008 than 2009 (Figure 4.3). Though less prominent, a similar pattern of higher productivity in 2008 was observed over seasonal averages of the Chl a standing

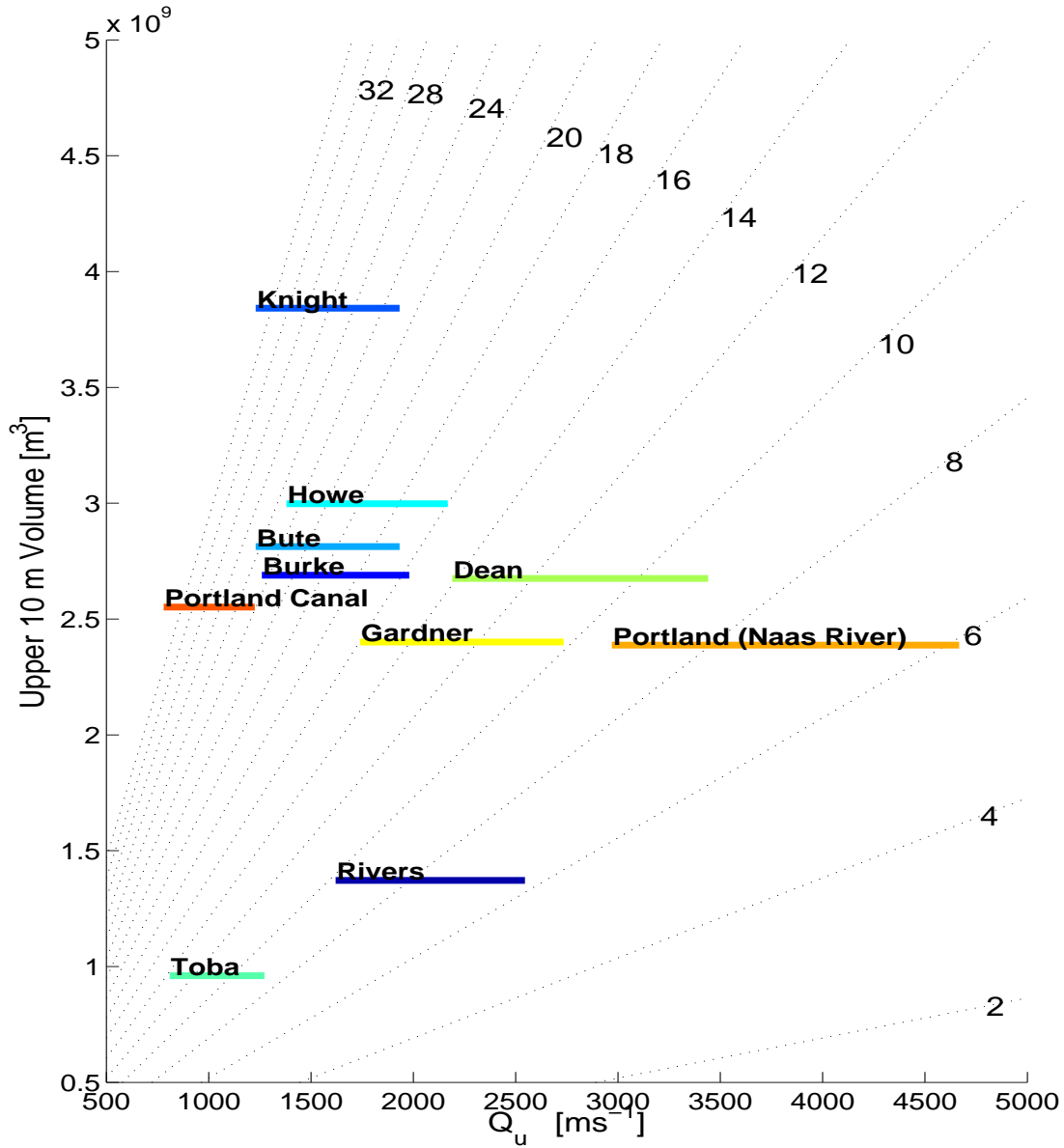


Figure 5.1: Comparing upper residence time estimates for several highly-stratified estuaries along the British Columbia mainland coast. Dashed lines indicate lines of constant residence time in days.

stock. The generally lower estimate of productivity in 2009 could have several causes. The deep water renewal event observed in 2009 was later and weaker. Deep water renewal is the primary mechanism that supplies and controls overall nutrient levels in estuaries (Thomson, 1981). Weaker renewal in 2009 caused lower supply rates and nutrient levels in the bottom layer, resulting in lower new production estimates during this time.

Lower seasonal productivity in 2009 may also be explained by changes in surface residence time during the spring. In 2009 a significant drop in surface residence times occurred at least two weeks earlier than in the previous year (Figure 4.2). Shorter surface residence times means higher surface advection rates. Higher surface advection rates during spring have been recently suggested as an important factor that may inhibit phytoplankton blooms (Wolfe, 2010) and overall lower-trophic level productivity in the inlet (Tommasi et al., 2010). Therefore, an earlier drop in residence times during the spring may introduce a shorter window of opportunity for favorable conditions resulting in lower phytoplankton growth.

Long Term Trend

Figure 5.2 shows an empirical relationship between upper residence times and river discharge. The trend indicates that residence times, while increasing with river discharge, do so hyperbolically. This means that surface residence times were more sensitive to changes at lower discharge values, and therefore can highlight important features that may be missed in a direct analysis of river discharge.

Using this relationship, the 49 year record of daily river discharge values was converted to residence times (Figure 5.3a). An interesting feature was the amount of interannual variability that occurs around the spring period. In some years (eg. 1994, 1996), shorter (<7 days) residence times start to appear before yearday 110, whereas in other years (eg. 1977, 1984) these values are not recorded until around yearday 160.

To examine the long term trend, the first yearday for which surface residence times dropped below 7 days in the spring was plotted for each year (Figure 5.3b). This measure was a very good indicator of the onset of the freshet. Results showed a significant decreasing trend of about 10 days over the last 50 years. This trend implies that Rivers Inlet is experiencing an earlier start to higher advection rates in the surface layer than it did in the past.

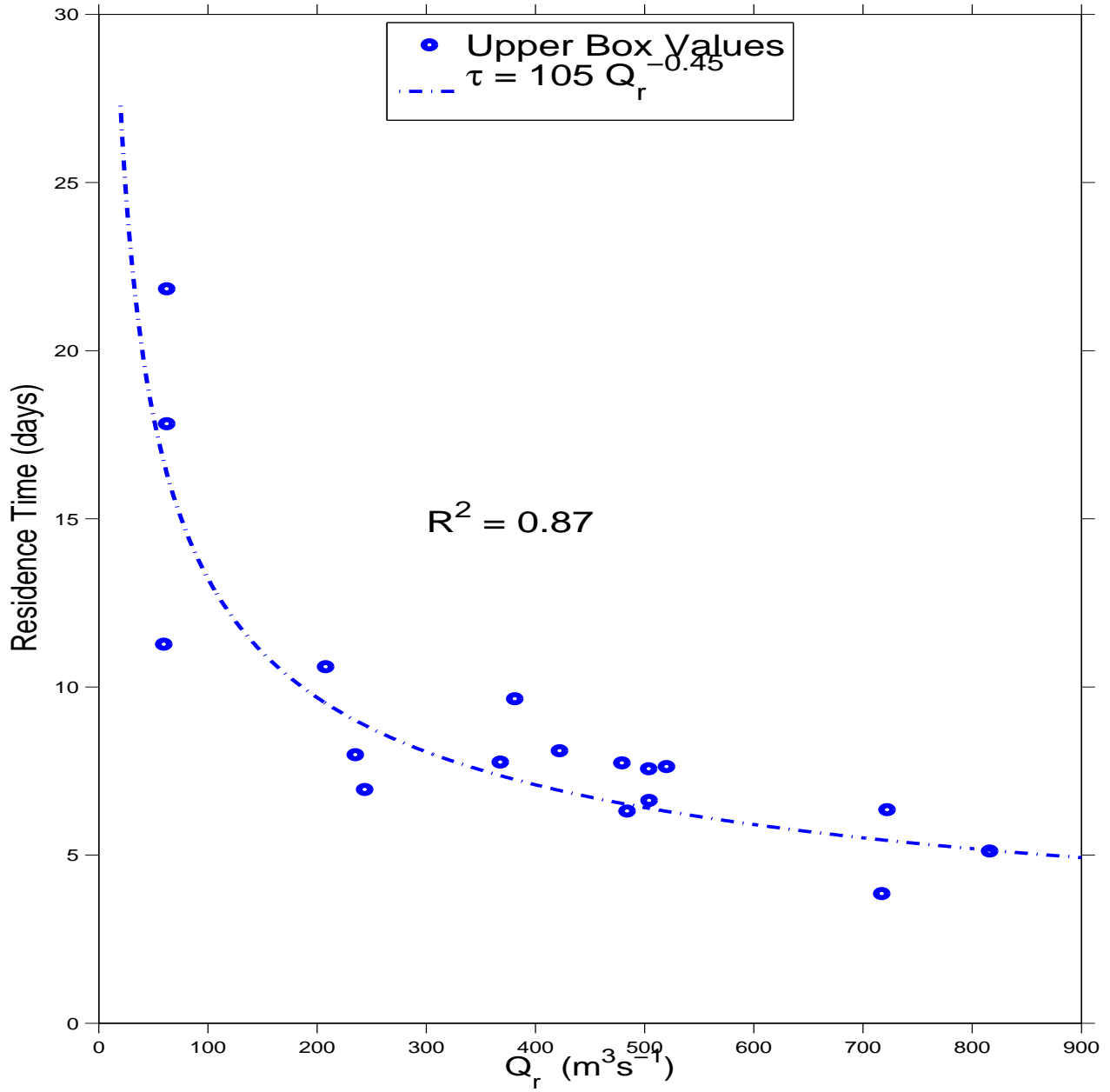


Figure 5.2: Upper box residence times as a function of river discharge. The circles are direct estimates from Figure 4.2a.

The timescale of an earlier shift by about 10 days over the last 50 years is synonymous with the general trend towards earlier spring development along this coast (Beaubien and Freeland, 2000). If the pattern of earlier drop in residence times with lower production we have seen in 2008 and 2009 hold true for the rest of the 50 year record, and assuming that light levels during this time remained the same, this would imply that the conditions for lower trophic-level production are less favorable now than they were in the past. Of course this view is rather oversimplified because it does not take into account other factors such as wind variations that happen at the same time. Wind variations (Wolfe, 2010), as well as light levels (Tommasi et al., 2010) are potentially important and could modify this picture and should be looked at in future work.

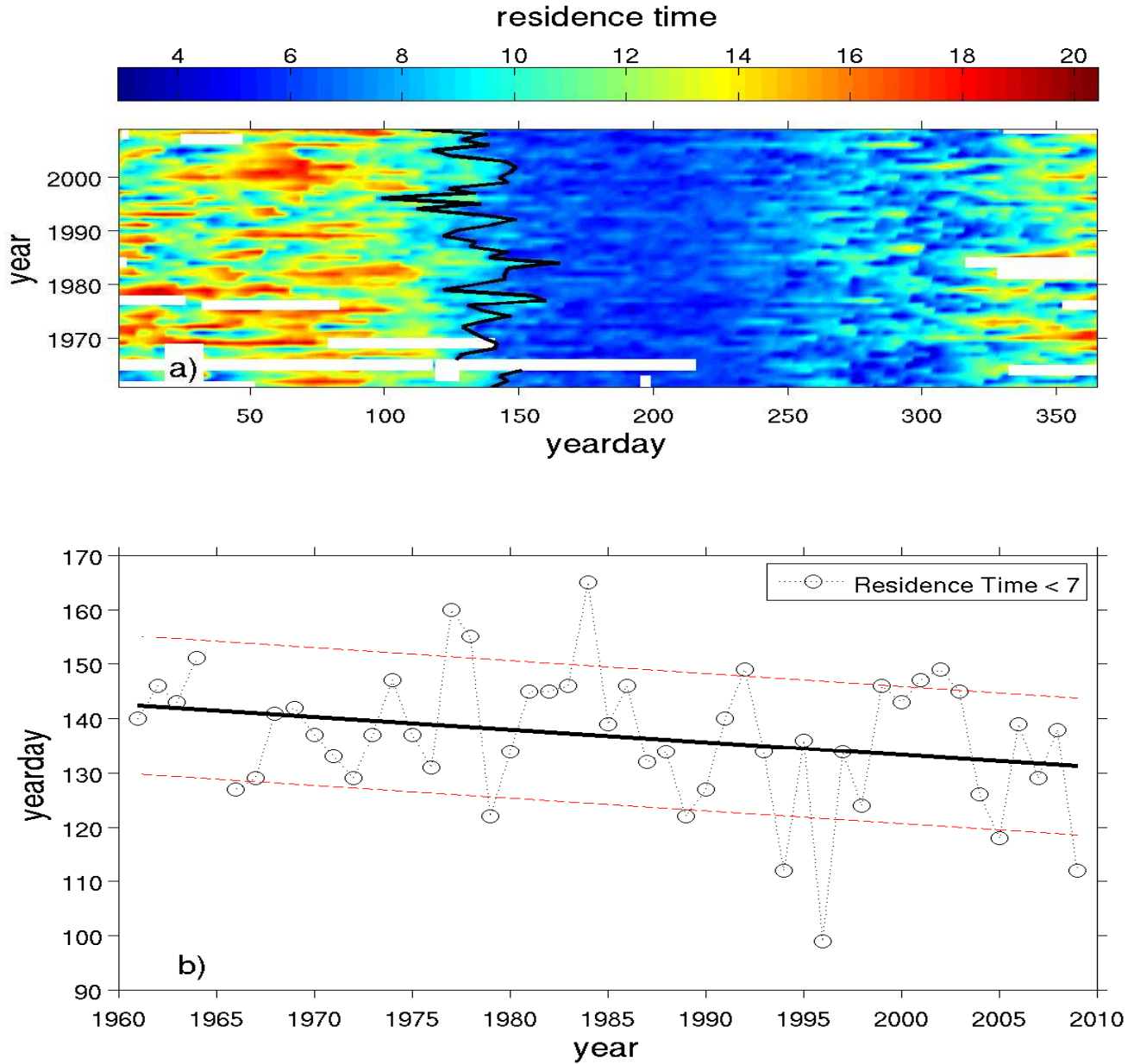


Figure 5.3: (a) Daily fitted residence times from river discharge measurements for the entire 49 year record; (b) first yearday when residence times drops below 7 days.

Chapter 6

Summary and Next Steps

In this thesis, I have presented and analyzed observations of water column properties and atmospheric variables using a recently collected dataset in a remote coastal fjord over the span of two-years. The water column observations clearly reveal a dominant two-layer structure to the system. In the summer months, when river discharge was high, vertical water column salinity increases from 2 at the surface to 33 at 5 m were observed as far as 30 km down estuary (Figure 2.5).

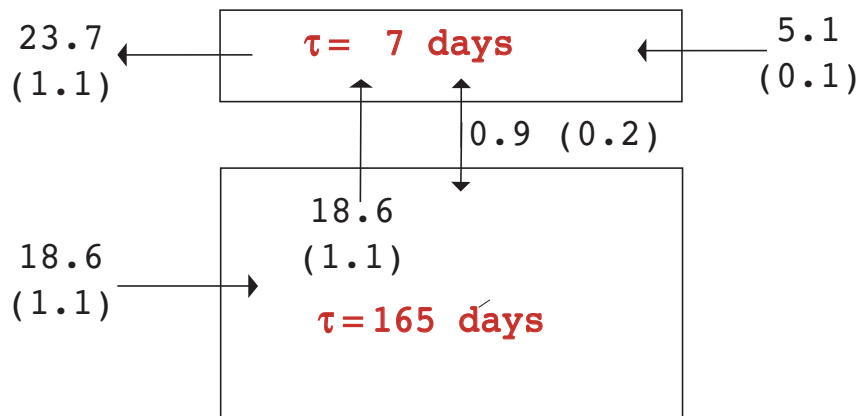
The flow in the Wannock River, which is the main source of freshwater input into Rivers Inlet, increased by an order of magnitude in early spring (due to glacial melt) and remained high ($\sim 560 \text{ m}^3\text{s}^{-1}$) throughout the summer and into early fall. Another large peak in flow occurs around October and November and was strictly due to runoff from increased precipitation.

The net air-sea heat flux observations were well correlated with water temperatures in the surface layer. The net air-sea heat flux had a seasonal range of approximately 220 Wm^{-2} and peaked almost a month earlier in 2008 than in 2009. Peak values were higher in 2009 (170 Wm^{-2}) than in 2008 (107 Wm^{-2}). The annual heat flux mean was estimated at 10 Wm^{-2} into the inlet and this value compares well with nearby estimates.

First estimates of transport, described as residence times, were obtained from conservation equations of mass and tracer balance in an idealized box model. Estimates of residence times were made for each hydrographic survey where sufficient data was available. Residence times for the upper box varied by a factor of two; averaging to about 7 and 16 days during periods of high and low river discharge, respectively (Figure 6.1). Residence times for the lower box during the summer averaged to about 150 days. Given the observed summer renewal period of approximately 4 months, the estuary is well replenished, with almost complete renewal occurring about once a year.

Transport estimates were merged with observed concentrations of nitrate to estimate rates of new production in the inlet by quantifying nitrate sinks. The average two-year estimate of $0.6\text{-}1.7 \text{ gCm}^{-2}\text{d}^{-1}$ (or assuming half-a-year

a) High River
Discharge



b) Low River
Discharge

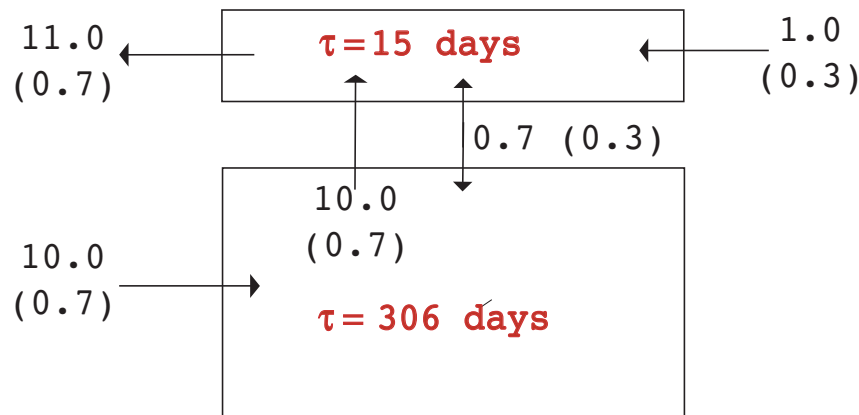


Figure 6.1: Summary of transport estimates and residence times for Rivers Inlet: a) during periods of high river discharge and deep water renewal (summer) and b) during winter. Flux estimates are in units $\times 10^2 \text{ m}^3 \text{ s}^{-1}$ and bootstrap error values are in brackets.

production about $110\text{-}300\text{ gCm}^{-2}\text{y}^{-1}$) was consistent with independent production estimates of nearby systems. This, in addition to consistent comparisons with independent estimates using a temperature budget, increased the level of confidence of our calculation. Other studies attempting to estimate primary production directly in the inlet are now in progress and should provide additional insight into the accuracy of our estimates.

Finally, we have shown evidence suggesting that residence times may be important physical and biological control for this estuary. An earlier drop in surface residence times in 2009 coincided with lower seasonal production. If this and the observed long term trend of increasing periods of lower surface residence times hold true, this could mean that current conditions are less favourable for lower-trophic production, and possibly marine survival of the Rivers Inlet sockeye (Ainsworth et al., 2010). However, a more complex model is required to include effects of wind speed and direction (Wolfe, 2010), as well as light levels (Tommasi et al., 2010) which appear to be important and could modify this picture. A more complex study may mean developing a prognostic box-model of estuarine circulation in Rivers Inlet, and coupling it with, for example, the Rivers Inlet bio-physical model of Wolfe (2010). Similar methods have been implemented in the Strait of Georgia (Li et al., 2000) and may prove useful for this system.

Bibliography

Anderson, J., Devol, A., 1973. Deep water renewal in Saanich Inlet, an intermittently anoxic basin. *Estuarine and Coastal Marine Science* 1, 1–10.

Beaubien, E., Freeland, H., 2000. Spring phenology trends in Alberta Canada: links to ocean temperature. *International Journal of Biometeorology* 44, 53–99.

Beaugrand, G., Brander, K., Lindley, J., Souissi, S., Reid, P., 2003. Plankton effect on cod recruitment in the north sea. *Nature* 426 (11), 661–664.

Buchanan, S. L., 2007. Factors influencing the early marine ecology of juvenile sockeye salmon (*Oncorhynchus nerka*) in Rivers Inlet, British Columbia. Ph.D. thesis, Simon Fraser University, Burnaby, Canada.

Dickey, T., Manov, D., Weller, R., Siegel, D., 1994. Determination of long-wave heat flux at the air-sea interface using measurements from buoy platforms. *J. Atmos. Oceanic Tech.* 11, 1057–1076.

Dyer, K. R., 1974. The salt balance in stratified estuaries. *Estuarine and Coastal Marine Science* 2, 275–281.

Dyer, K. R., 1991. Circulation and mixing in stratified estuaries. *Marine Chemistry* 32, 111–120.

Dyer, R. K., 1997. *Estuaries: A Physical Introduction*, 2nd Edition. John Wiley and Sons.

Eppley, W., Peterson, B., 1979. Particulate organic matter flux and planktonic new production in the deep ocean. *Nature* 282, 677–680.

Farmer, D., Freeland, H., 1983. The physical oceanography of fjords. *Progress in Oceanography* 12, 147–220.

- Gordon Jr, D. C., Boudreau, P. R., Mann, K. H., Ong, J. E., Silvert, W. L., Smith, S. V., Wattayakorn, G., Wulff, F., Yanagi, T., 1996. Loicz biogeochemical modelling guidelines. Tech. rep., LOICZ/R&S/95-5, VI+ 96 PP.
- Hagy, J. D., Boynton, W. R., Sanford, L., 2000. Estimation of net physical transport and hydraulic residence times for a coastal plain estuary using box models. *Estuary Research Federation* 23 (3), pp. 328–340.
- Harrison, P., Fulton, J., Taylor, F., Parsons, T., 1983. Review of the biological oceanography of the Strait of Georgia: pelagic environment. *Can. J. Fish. Aquat. Sci.* 40, 1064–1094.
- Hodgins, D., 1979. A time-dependent two-layer model of fjord circulation and its application to Alberni Inlet, British Columbia. *Estuarine and Coastal Marine Science* 8, 361–378.
- Legendre, L., Rassoulzadegan, F., Michaud, J., 1999. Identifying the dominant process (physical versus biological) in pelagic marine ecosystems from field estimates of chlorophyll a and phytoplankton production. *Journal of Plankton Research* 21 (9), 1643–1658.
- Levy, D., 2006. BC sockeye salmon population declines: Probable causes and recommended response strategies. Prepared for: The Sierra Club of Canada - BC Chapter.
- Li, M., Gargett, A., Denman, K., 1999. Seasonal and interannual variability of estuarine circulation in a box model of the Strait of Georgia and Juan de Fuca Strait. *Atmosphere Ocean* 37, 1–19.
- Masson, D., 2002. Deep water renewal in the Strait of Georgia. *Estuarine, Coastal and Shelf Science* 54, 115–126.
- McKinnell, S. M., Wood, C. C., Rutherford, D. T., Hyatt, K. D., Welch, D. W., 2001. The demise of owikeno lake sockeye salmon. *North American Journal of Fisheries Management* 21 (4), 774–791.
- Mueter, F. J., Peterman, R. M., Pyper, B. J., 2002. Opposite effects of ocean temperature on survival rates of 120 stocks of pacific salmon (*Oncorhynchus* spp.) in northern and southern areas. *Canadian Journal of Fisheries and Aquatic Sciences* 59 (3), 456–463.

-
- Officer, C. B., 1980. Box models revisited. *Estuarine and Wetland Processes, with Emphasis on Modeling* 11, 65–114.
- Pawlowicz, R., 2001. A tracer method for determining transport in two-layer systems, applied to the Strait of Georgia/Haro Strait/Juan de Fuca Strait estuarine system. *Estuarine, Coastal and Shelf Science* 52 (4), 491–503.
- Pawlowicz, R., Beardsley, B., Lentz, S., Dever, E., Anis, A., 2001. Software simplifies air-sea estimates. *EOS Trans. Amer. Geophys. Union*.
- Pawlowicz, R., Farmer, D. M., 1998. Diagnosing vertical mixing in a two-layer exchange flow. *Journal of Geophysical Research-Oceans* 103 (C13), 30695–30711.
- Pawlowicz, R., Riche, O., Halverson, M., 2007. The circulation and residence time of the Strait of Georgia using a simple mixing-box approach. *Atmosphere-Ocean* 45 (4), 173–193.
- Payne, R. E., 1972. Albedo of the sea surface. *J. Atmos. Sci.* 29, 959–970.
- Pickard, G., 1961. Oceanographic features of inlets in the British Columbia mainland coast. *Journal of the Fisheries Research Board of Canada* 18 (6), 907–999.
- Pickard, G., 1963. Oceanographic characteristics of Inlets of Vancouver Island, British Columbia. *Journal Fishers Research Board of Canada* 20 (5), 1109–1144.
- Sarmiento, J., Gruber, N., 2006. *Ocean Biogeochemical Dynamics*. Princeton University Press.
- Sheldon, E., Alber, M., 2005. Comparing transport times through salinity zones in the ogeechee and altamaha river estuaries using squeezebox. *Proceedings of the 2005 Georgia Water Resources Conference*.
- Stacey, M., 1985. Some aspects of the internal tide in Knight Inlet, British Columbia. *Journal of Physical Oceanography* 12, 1652–1661.
- Stacey, M., Pond, S., Nowak, Z., 1994. A numerical model of the circulation in Knight Inlet, British Columbia, Canada. *American Meteorological Society* 25, 1037–1062.

-
- Strickland, J., Parsons, T., 1972. A practical handbook of seawater analysis, second ed. Bull. Fish. Res. Board Can., 167.
- Thomson, R., 1981. Oceanography of the British Columbia coast. Canadian Special Publication of Fisheries and Aquatic Sciences 56, 291.
- Timothy, D., Soon, M., 2000. Primary production and deep-water oxygen content of two British Columbian fjords. Mar. Chem. 73, 37–51.
- Tommasi, D., Routledge, R., Hunt, B., Pakhomov, E., 2010. Spring phytoplankton bloom dynamics in a fjord on the central coast of British Columbia. Canadian Journal of Aquatic Sciences, in press.
- Ware, D., McQueen, D., 2006b. Hecate Strait climate-forced nutrient, phytoplankton, zooplankton model version 4.3.4. Canadian Technical Report of Fisheries and Aquatic Science 2653.
- Ware, D. M., Thomson, R. E., 2005. Bottom-up ecosystem trophic dynamics determine fish production in the Northeast Pacific. Science 308 (5726), 1280.
- Wolfe, A., 2010. Impact of wind and river flow on the timing of the Rivers Inlet spring phytoplankton bloom. Master's thesis, University of British Columbia, Vancouver, Canada.
- Wright, D. G., Pawlowicz, R., McDougall, T. J., Feistel, R., Marion, G. M., 2010. Absolute salinity, "density salinity" and the reference-composition salinity scale: present and future use in the seawater standard teos-10. Ocean Science Discussions 7 (4), 1559–1625.
URL <http://www.ocean-sci-discuss.net/7/1559/2010/>

Appendix A

Heat Flux

The net heat flux across the air–water interface, H , can be decomposed into four component heat fluxes, namely:

$$H = q_s + q_b + q_h + q_e \quad (\text{A.1})$$

where q_s is the net incoming shortwave solar radiation, q_b is the effective longwave radiation, q_h is the sensible heat flux or direct conduction at the water surface, and q_e is the latent heat flux of evaporated water, all in Wm^{-2} . Each of these fluxes were computed using the Air-Sea MATLAB toolbox¹, and will be described, in turn:

Net shortwave flux is calculated using

$$q_s = (1 - a) \cdot dsw \quad (\text{A.2})$$

where a is the albedo and dsw is the *in situ* downwelling shortwave radiation. The albedo a is estimated from date, atmospheric transmittance, and geographic parameters following Payne (1972).

The **net longwave flux** can be computed directly using sea surface temperature, T_s units Kelvin, measured downward longwave flux, dlw , and dsw as defined previously. In general, the relation is given by

$$q_b = 0.985(dlwc - \sigma T_s^4) \quad (\text{A.3})$$

where 0.985 is the long-wave emissivity of ocean constant from Dickey et al. (1994), σ is the Stefan-Boltzmann constant, and $dlwc$ is the corrected dlw for sensor heating by insolation given by $dlwc = dlw - 0.025 \cdot dsw$ as required for Kipp & Zonen CG1 pyrgeometers used in this study.

The **sensible and latent heat fluxes** are estimated using bulk formulae relating wind stress, and a number of other parameters. In their most

¹The toolbox is available via the World Wide Web at the SEA-MAT site maintained by Rich Signell of the U.S. Geological Survey (<http://crusty.er.usgs.gov/sea-mat/>).

common form, these turbulent fluxes may be written as

$$q_h = \rho_a C_{pa} C_H W (T_s - T_a) \quad (\text{A.4})$$

$$q_e = \rho_a L C_e W [q(T_s) - q_d] \quad (\text{A.5})$$

where T_a is the surface air temperature, W is the wind speed at 10 m, q is the saturation specific humidity at T_s , q_d is the saturation specific humidity at the dew point temperature at 10 m, C_e and C_h are the bulk transfer coefficients of moisture and heat, respectively, ρ_a is air density, and L is the latent heat of vaporization of water in units Jkg^{-1} given by $L = 2.501 \cdot 10^6 - 2.37 \cdot T_s$.

Appendix B

RIES Weather Station

This section provides a summary of sensors and sampling rates for the RIES meteorological dataset. From February 2008 to February 2009, the dataset consists of the following measurements made by the “Ethel” station (SFU) at an interval of 10 minutes:

- Wind: Speed and Direction
- Temperature
- Solar Radiation

In March 2009, the existing “Ethel” station was replaced by “Laska” to measure a more complete set of meteorological parameters required in heat budget analysis (Section 2.2). The names of sensors and logging parameters for Laska are summarized in Table B.1. The measurements were programmed to sample at 1 minute intervals and log the mean every 15 minutes.

Sensor	Measurement	Units	Accuracy
05106 R.M Young Wind Monitor	Wind Speed	$\frac{m}{s}$	$\pm 0.3 \frac{m}{s}$
	Wind Direction	θ	$\pm 0.3^\circ$
HOBO Pro v.2	Temperature	$^\circ C$	$\pm 0.2 \text{ }^\circ C$
	Relative Humidity	%	$\pm 2.5 \%$
Kipp & Zoen CG1 Pyrgeometer	Long Wave Radiation	$\frac{W}{m^2}$	$< 20 \frac{W}{m^2}$
Kipp & Zoen CMP3 Pyranometer	Short Wave Radiation	$\frac{W}{m^2}$	$< 20 \frac{W}{m^2}$
TE525 MM Bucket Rain Gauge	Precipitation	mm	$\pm 1 \%$

Table B.1: Summary of Sensors for Laska and now the RIES weather station.

Appendix C

Catchment Area Calculations

Relative percentages of freshwater input from ungauged catchments were estimated using regional analysis. Regional analysis of catchment areas and characteristics were marked out using ImapBC. ImapBC is a multi-use online resource (<http://webmaps.gov.bc.ca/imfx/imf.jsp?site=imapbc>) that uses the Land and Resource Data Warehouse (LRDW), a consolidated repository of land and resource information from across the province, and is maintained by The Integrated Land Management Bureau. Annual yield (Q) for ungauged (u) catchments (Areas 2-4 in Figure 2.1) were estimated from a ratio of catchment areas (A) with gauged (g) catchments using: $Q_u/A_u = Q_g/A_g$. Sensible use of this relation requires making the assumption that the catchment being estimated has similar precipitation and runoff characteristics as the gauged counterpart. The assumption that all catchments have similar characteristics holds true more for Area 1 and 2 than for Area 2 and 3. Still, the annual yield of 2.54 my^{-1} was reasonable and relatively consistent with large scale average precipitation curves (Figure 2.1).

Appendix D

Monthly Heat Flux Averages

	Shortwave (q_s)	Longwave (q_b)	Sensible (q_h)	Latent (q_e)	Net Heat Flux(H)
Mar 08	90.21	n/a	n/a	n/a	-13
Apr 08	141.80	n/a	n/a	n/a	38
May 08	208.22	n/a	n/a	n/a	105
Jun 08	182.22	n/a	n/a	n/a	79
Jul 08	164.30	n/a	n/a	n/a	61
Aug 08	150.84	n/a	n/a	n/a	47
Sep 08	122.69	n/a	n/a	n/a	19
Oct 08	54.08	n/a	n/a	n/a	-49
Nov 08	25.54	n/a	n/a	n/a	-78
Dec 08	14.29	n/a	n/a	n/a	-89
Jan 09	17.84	n/a	n/a	n/a	-86
Feb 09	62.41	n/a	n/a	n/a	-41
Mar 09	86.63	-82.90	-13.58	-26.59	-36
Apr 09	133.94	-88.89	-1.44	-13.85	30
May 09	n/a	n/a	n/a	n/a	92
Jun 09	219.60	-66.67	2.77	-1.26	170
Jul 09	240.64	-72.16	4.03	-2.25	154
Aug 09	171.74	-71.07	-1.27	-13.68	86
Sep 09	101.22	n/a	n/a	n/a	-3
Oct 09	69.59	n/a	n/a	n/a	-34
Nov 09	22.54	n/a	n/a	n/a	-81
Dec 09	16.98	n/a	n/a	n/a	-87
Jan 10	18.81	n/a	n/a	n/a	-85
Feb 10	55.50	n/a	n/a	n/a	-48
Mar 10	87.71	-74.18	1.17	-17.56	-3
Apr 10	152.14	-92.15	-11.02	-30.92	18
May 10	194.64	-95.19	-12.85	-35.97	51
June 10	170.87	-76.21	-9.71	-28.21	57

Table D.1: Summary of monthly averages for all components of the air-sea heat flux of Figure 2.3 (Section 2.2). Gaps (especially in the winter months) were due to lack of surface temperature data. The net heat flux (H) was estimated using linearly interpolated values.

Appendix E

Hypsometric Curves

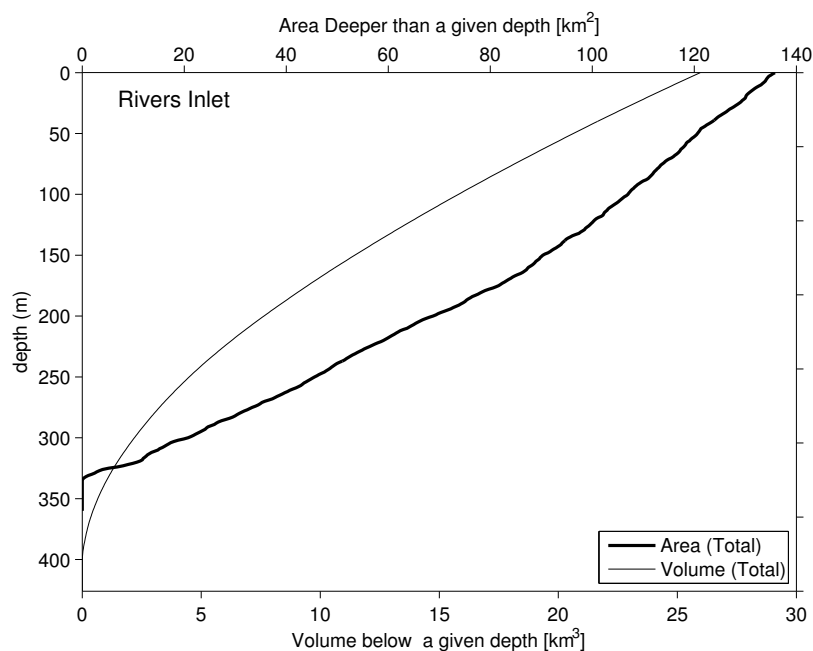


Figure E.1: Hypsometric curve for Rivers Inlet showing area (bold line) and volume (thin line) as a function of depth. The estimated mean-low-water volume and surface area is $25.96 \times 10^9 \text{ m}^3$ and $135.80 \times 10^6 \text{ m}^2$, respectively. These curves were calculated using cumulative trapezoidal numerical integration of a 2×2 minute bathymetric grid database from the National Geophysical Data Center (<http://dss.ucar.edu/datasets/ds759.3/>).